

## SUPPLEMENTAL INFORMATION

### Development of Novel Glucocorticoids for Use in Antibody Drug Conjugates for the Treatment of Inflammatory Diseases

Amy Han\*, Olav Olsen, Christopher D'Souza, Jing Shan, Feng Zhao, Jean Yanolatos, Zaruhi Hovhannisyan,  
Sokol Haxhinasto, Frank Delfino, and William Olson

Regeneron Pharmaceuticals, Inc., Tarrytown, NY 10591, United States

Amy Han [amy.han@regeneron.com](mailto:amy.han@regeneron.com) (\*Correspondence)

#### Contents

1. Modeling of Glucocorticoid (GC) in complexes with Glucocorticoid Receptor (GR) (3D modeling results of the GCs in GR are available in separate PDB PYMOL files)
2. Separation and structural determination of chiral Glucocorticoids (GCs): 1) SFC conditions, 2) analytical and preparative HPLC methods and conditions, 3) Structural determination of *R*-epimer vs *S*-epimer of GCs by NOESY and 4) NMR of chiral GCs, 5) LC-MS spectra of all payloads and linker-payloads
3. ESI-MS Spectra of site-specific antibody drug conjugates (ADCs)
4. In vitro bioassays: 1) Cell-free GR binding assay, 2) A panel of cell-free nuclear receptors (NRs) binding assays, 3) Cell-based reporter assay and 4) Bystander effect assay
5. ADME assays: 1) Plasma stability, 2) Caco2 assay and 3) Cathepsin B enzymatic assay
6. In vivo mouse model of LPS-induced TNF $\alpha$  release
7. Pharmacokinetic study protocol
8. Structures with SMILE formula strings
9. References

## 1. Modeling of Glucocorticoid (GC) in Complexes with Glucocorticoid Receptor (GR)

### 1.1 Method

The binding modes of each pair of 22*R*- and 22*S*-epimers of **P3** and **P12** with the GR were modeled using Schrödinger Drug Discovery Suite 2017.<sup>1</sup> The co-crystal structure of the GR complexed with *R*-desisobutyrylciclesonide (PDBID: 4UDD) was selected as the receptor structure and prepared using Protein Preparation Wizard. During protein preparation, only waters 2044 and 2084 located in the binding site were kept and all other water molecules were removed. The structures of all epimers of **P3** and **P12**, and original ligand in 4UDD (*R*-desisobutyrylciclesonide) are shown in Figure S1. Possible ionization states were generated at pH 7.0±1.0 and the primary amine group of **P3** was protonated. All epimers of **P3** and **P12** were prepared using LigPrep and were docked into 4UDD, using Induced Fit Docking, with the box centered to the centroid of the ligand. The most possible binding poses were selected and shown using PyMOL.<sup>2</sup>

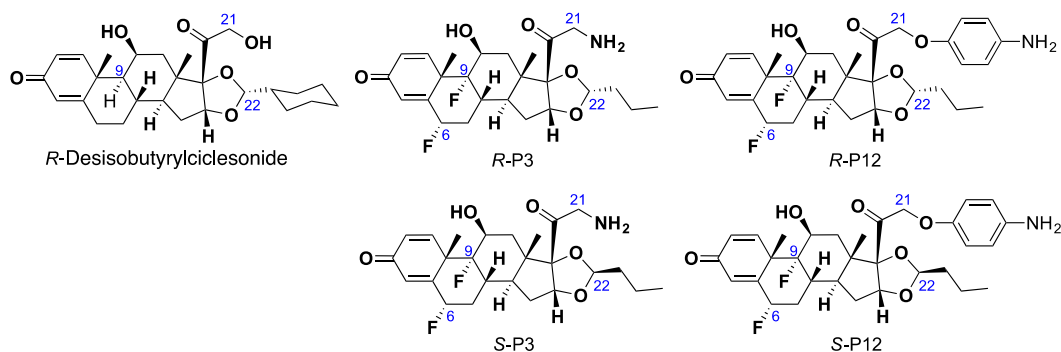


**Figure S1.** Chemical structures of 22*R*- and 22*S*-epimers of **P3** & **P12**, and *R*-desisobutyrylciclesonide

### 1.2 Results

The predicted binding modes of 22*R*- and 22*S*-epimers of **P3** and **P12** based on the docking results are shown in Figures S2 to S6, indicating their potential interactions with the GR through hydrogen-bonding, cation- $\pi$  interactions or  $\pi$ - $\pi$  interactions. In the figures, the GR is based on PDB:4UDD and shown as a transparent cartoon and key residues highlighted with all carbon atoms of the GR in grey and all ligands

(**P3**, **P12**, and *R*-desisobutyrylciclesonide) as ball and sticks. In addition, all nitrogen atoms are in blue, oxygen atoms in red, sulfur atoms in yellow, fluorine atoms in light blue and polar hydrogen atoms in white. Hydrogen bonds and water-bridged hydrogen bonds between ligand and receptor are shown as yellow dash lines.

The GR docking model of *R*-**P3** fits well in the active site of the GR, resulting in the formation of a complex network of hydrogen bonds interactions for *R*-**P3** with GR (Figure S2). Key interactions indicated are the C<sup>3</sup> carbonyl oxygen with Gln570 and Arg611, the C<sup>11</sup> hydroxyl with Asn564, one oxygen atom (near C<sup>16</sup>) of the dioxolane ring via a water molecule with Gln642 and the C<sup>21</sup> protonated amine group with Thr739, Asn564.

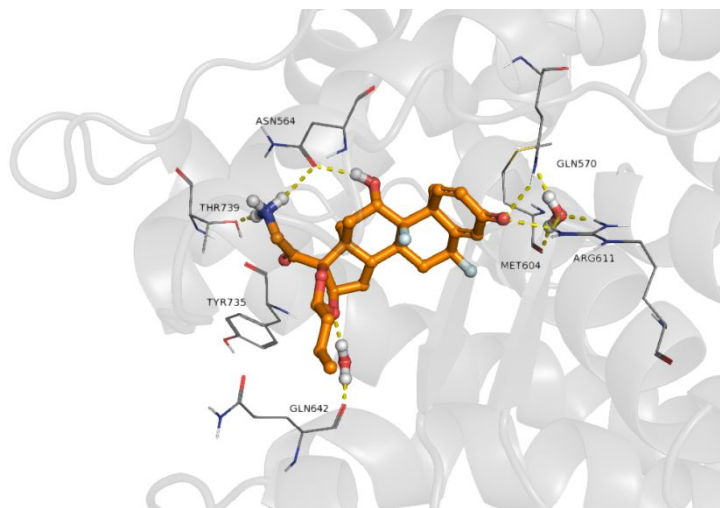


**Figure S2.** Predicted binding mode of *R*-**P3** (in orange) with the GR in gray.

Superpositioning 22*R*- and 22*S*-epimers of **P3** (Figure S3) indicate that all binding modes are identical, except for the small conformational change around the propyl group, as well as, altered configurations of the dioxolane ring (that is discussed in the section of structural determination).

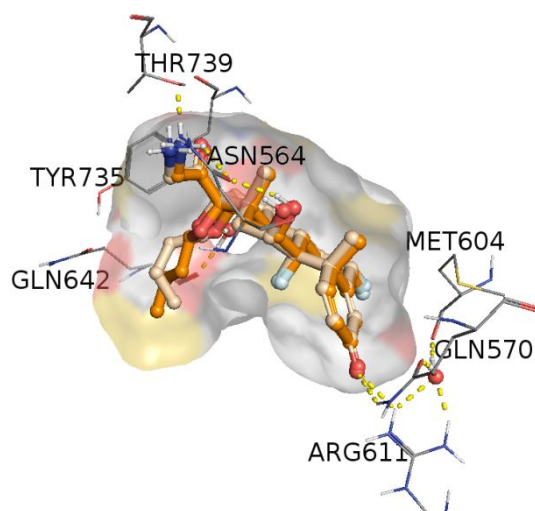


**Figure S3.** Superposition of *R*-**P3** (in orange) and *S*-**P3** (in yellow) docked in active site of the GR using 4UDD; the GR surface in gray.

The 22*R*-epimer of **P12** is predicted to have two possible binding poses with the aniline group pointing in two different directions (Figure S4). In both binding poses, the C<sup>3</sup>-carbonyl oxygen forms hydrogen bonds with Gln570 and Arg611, C<sup>11</sup>-hydroxyl group forms a hydrogen bond with Asn564, and one of the oxygen atoms (near C<sup>16</sup>) on the dioxolane ring forms a water-bridged hydrogen bond with Gln642. In pose “a” (Figure S4a), the C<sup>20</sup>-carbonyl oxygen and the C<sup>21</sup>-aryloxy oxygen form hydrogen bonds with Thr739. The aniline moiety forms hydrogen bonds with Thr561 and Ser746. In pose “b” (Figure S4b), the aniline moiety forms a hydrogen bond with Gln738, and a  $\pi$ - $\pi$  interaction with Tyr735. The strain energy of the two poses are 2.07 kcal/mol and 4.12 kcal/mol, respectively. Thus, pose “a” is preferred. The difference between binding of *R*-**P12** and *R*-desisobutyrylciclesonide in the GR active site is that the aniline moiety of *R*-**P12** extends within the binding pocket and makes additional hydrophobic interactions. The hydrogen bond interactions between Ser746 and Thr561 and aniline moiety of *R*-**P12** in pose “a” in the GR are predicted (Figures S4 and S5).

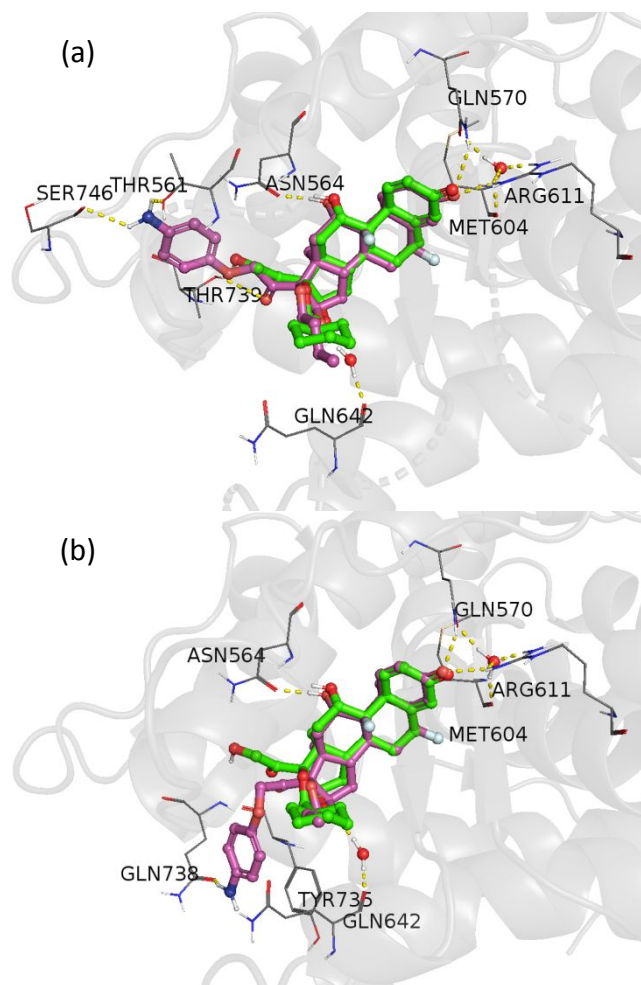


**Figure S4.** Predicted two binding modes (a & b) of 22*R*-epimer of **P12** (in purple) docked in binding pocket of crystal structure PDB-ID:4UDD (R-desisobutyrylciclesonide in green and GR in gray) within the GR binding site.

Superposition of the 22*R*- and 22*S*-epimers of **P12** in the binding site of the GR (Figure S5) indicates all binding modes are identical, except a small conformational change around the propyl group, and small different configurations of the dioxolane ring.

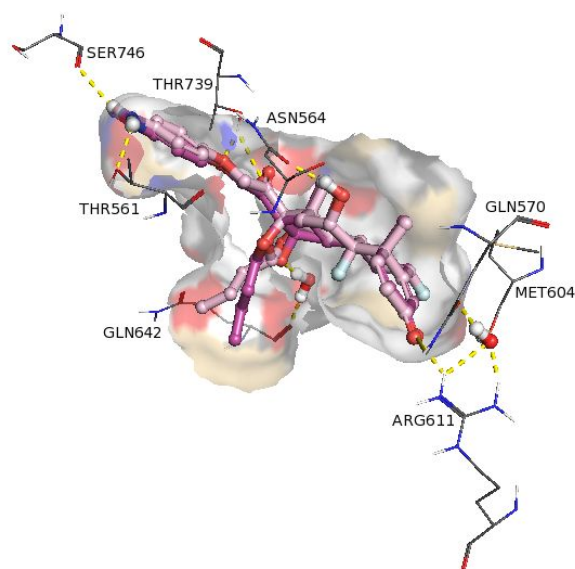


**Figure S5.** Predicted GR surface around *R*-**P12** (in purple) and *S*-**P12** (in pale pink) superposition in the GR active site.

Both 22*R*-epimers of **P3** and **P12** are predicted to have similar binding modes to that of original ligand in 4UDD, as indicated by superposition of *R*-**P3**, *R*-**P12** (two poses), and *R*-desisobutyrylciclesonide (Figure S6). Recently, the crystal structure of *S*-Budesonide complexed with the GR (PDB:5NFP) was reported.<sup>3</sup> Our modeling results closely agree with the findings for PDB:5NFP and do not impact the results and conclusions made in this report.

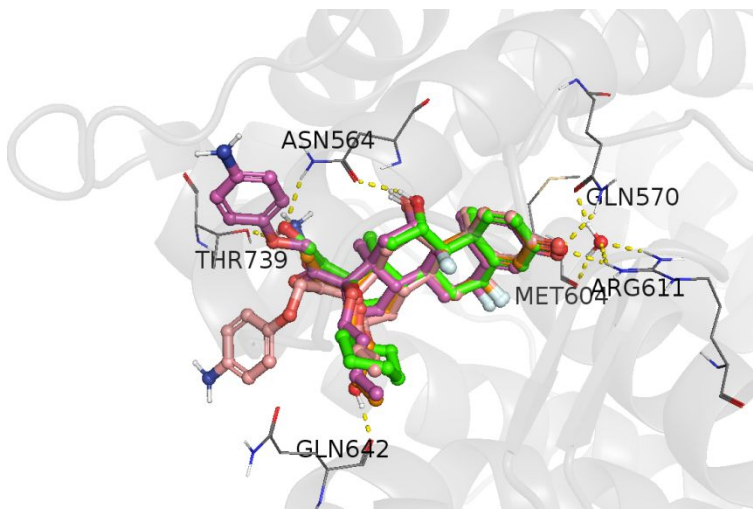


**Figure S6.** Superposition of *R*-**P3** (in orange) and *R*-**P12** (two poses: “a” in peach and “b” in pink) and original ligand (*R*-desisobutyrylciclesonide in green) docked in the GR active site.

## 2. Separation and Structural Determination of Chiral GCs

### 2.1 Separation by SFC

Commercial Budesonide was provided as a mixture of *R*- and *S*-epimers at the C<sup>22</sup>-position, with both having similar pharmacological effects. However, *in-vitro* studies suggested that the *R*-epimer was 3-5 times more potent than the *S*-epimer with respect to its anti-inflammatory effects.<sup>4</sup> Racemic Budesonide has been separated to afford the *R*-C<sup>22</sup> and *S*-C<sup>22</sup> epimers and structural characterization of each listed. It is noted in most reports that the *R*- and *S*-epimers were not completely separated or were separated in small amounts and mixtures with various ratios (*R*-/*S*- = 9:1 and 1:1) were used for structural determination of each configuration.<sup>5</sup>

We utilized supercritical fluid chromatography (SFC) for the separation of the chiral enantiomers.<sup>6</sup> Four pairs of *R*- and *S*-epimers of Budesonide (**P1**), **P3**, **P10**, and **P12** were completely separated by chiral SFC using an AD-H column. 9 grams of each *R*- and *S*-epimers of Budesonide were isolated from 20 grams of Budesonide (89% yield). Detailed conditions are listed in Table S1. For comparison with the reference data, *R*-Budesonide (*R*-**P1**) and *S*-Budesonide (*S*-**P1**) were separated from the C<sup>22</sup> racemic mixtures in

99.8% purity as determined by HPLC using a Sephadex LH-20 column using chloroform-heptane-ethanol (20/20/1) as the mobile phase.

Compound	Budesonide ( <b>P1</b> ) and <b>P3</b>	<b>P10, P12</b>
Instrument	SFC-200 (Thar, Waters)	SFC-200 (Thar, Waters)
Column	AD-H 20*250mm, 5um (Dacel)	SC 20*250mm, 5um
Column temperature	35 °C	35 °C
Mobile phase	CO <sub>2</sub> / methanol (0.5% NH <sub>4</sub> OH) = 70/30	CO <sub>2</sub> / methanol (0.5% NH <sub>4</sub> OH) = 60/40
Flow rate	120 g/min	140 g/min
Back pressure	100 bar	100 bar
Detection wavelength	214 nm	214 nm
Cycle time	4.0 min	5.0 min
Sample solution	20g dissolved in 130 ml Methanol	10g dissolved in 130 ml Methanol
Injection volume	1.0 ml	0.5 ml

**Table S1.** SFC conditions for chiral separation of each pair of *R*- and *S*-epimers

## 2.2 Analytical and preparative HPLC methods and conditions

LC-MS measurements were run on Agilent 1200 HPLC/6100 SQ System with the follow conditions:

**Method A:** Mobile Phase A: Water (0.01% TFA) and Mobile Phase B: Acetonitrile (0.01% TFA). The Gradient elution was 5% B increasing to 95% B within 1.4 min, and then held @ 95%B for 1.6 min at a flow rate of 2.0 mL/min. Column: SunFire C18, 4.6 x 50 mm, 3.5 µm @ 50°C. The detectors: an ADC ELSD, DAD (214 nm and 254 nm), and a mass-selective detector (MSD ES-API). **Method B:** Mobile Phase A: Water (10 mM NH<sub>4</sub>HCO<sub>3</sub>) and Mobile Phase B: Acetonitrile. The Gradient elution was 5% B increasing to 95% B within 1.4min, and then held @ 95%B for 1.6 min at a flow rate of 2.0 mL/min. Column:



XBridge C18, 4.6 x 50 mm, 3.5  $\mu\text{m}$  @ 50°C. The detectors: an ADC ELSD, DAD (214 nm and 254 nm), and a mass-selective detector (MSD ES-API).

Preparative high-pressure liquid chromatography (Prep-HPLC) was performed on a Gilson GX-281 instrument. Two solvent systems were used. The acid solvent system (**Method A**) included a Waters Sunfire 10  $\mu\text{m}$  C18 column (100  $\text{\AA}$ , 250 x 19 mm). Solvent A for prep-HPLC was 0.05% TFA in water and solvent B was acetonitrile. A linear gradient that increased solvent B from 5% to 100% over 20 min at a flow rate of 30 mL/min was used. The basic solvent system (**Method B**) included a Waters Xbridge 10  $\mu\text{m}$  C18 column (100  $\text{\AA}$ , 250 x 19 mm). Solvent A for prep-HPLC was 10 mM ammonium bicarbonate ( $\text{NH}_4\text{HCO}_3$ ) in water and solvent B was acetonitrile. A linear gradient that increased solvent B from 5% to 100% over 20 min at a flow rate of 30 mL/min. was used.

Flash chromatography was performed on a Biotage instrument, utilizing an Agela Flash silica-CS column. Reversed phase flash chromatography was performed on a Biotage instrument, utilizing a Boston ODS or Agela C18 column, unless indicated otherwise.

### 2.3 Structural Determination of *R*-epimer vs *S*-epimer of GCs by NOESY

The X-ray structure of  $\text{C}^{225}$ -Budesonide (PDB:5NFP) in complex with the GR has been reported. [3] The configuration at  $\text{C}^{22}$  has a crucial influence on the resonances of the neighboring protons. [5] Compared to the reported  $^1\text{H}$  NMR data of *R*- and *S*-epimers of Budesonide, the first compound obtained from chiral SFC was determined to be the *R*-epimer (***R*-P1**), while the second was the *S*-epimer (***S*-P1**). The comparison of  $^1\text{H}$  NMR chemical shifts (ppm in  $\text{CDCl}_3$ ) of reported *R*-/*S*-Budesonide epimers and ***R*-P1** and ***S*-P1** isolated from SFC are shown in Table S2. The determination was also proved by 2D-NMR. In the NOESY spectrum, an interaction between the  $\text{C}^{22}$ -proton and the  $\text{C}^{16}$ -proton was observed in ***R*-P1** (Figure S7a), thus illustrating that these two protons are on the same side of the acetal ring, while this interaction is not observed for the ***S*-P1** (Figure S7b).

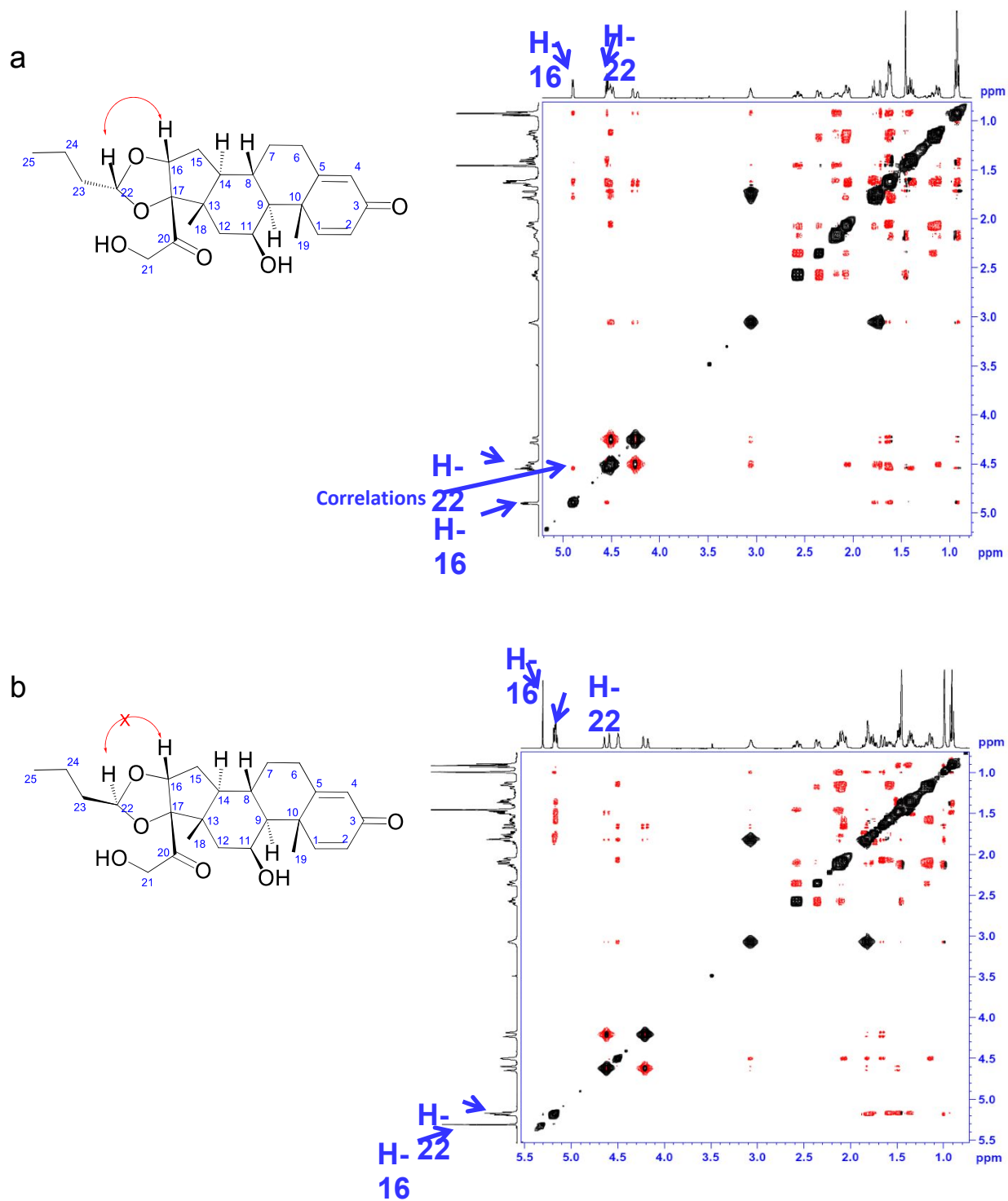
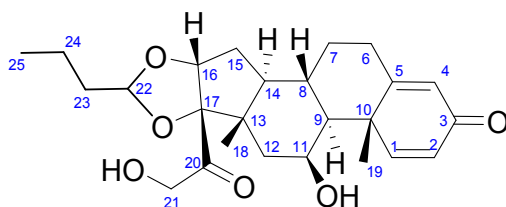


**Figure S7.** NOESY of *R*-P1 (a) and NOESY of *S*-P1 (b).

## 2.4 Side-by-side comparison of *R*- and *S*-epimers of P1, P3, P10, and P12 by $^1\text{H}$ NMR

The comparisons of  $^1\text{H}$  NMR chemical shifts are shown side-by side for *R*-**P1** and *S*-**P1** in Table S2, for *R*-**P3** and *S*-**P3** in Table S3, for *R*-**P10** and *S*-**P10** in Table S4, and for *R*-**P12** and *S*-**P12** in Table S5. The conformation of the dioxolane ring in the *S*- and *R*-epimers of **P1** is similar to that of the conformation of the ring in the *S*- and *R*-epimers of **P3**, **P10**, and **P12**, where the  $\text{C}^{22}$ - and  $\text{C}^{16}$ -protons in the *S*-epimers of **P1**, **P3**, **P10**, and **P12** being deshielded compared to the *R*-epimers of **P1**, **P3**, **P10**, and **P12**. In general, the average chemical shift of  $\text{C}^{22}$  protons are  $\sim 5.21\text{ppm}$  for the *S*-epimers and  $\sim 4.69\text{ppm}$  for the *R*-epimers; and the average chemical shift of  $\text{C}^{16}$  protons are  $\sim 5.16\text{ppm}$  for the *S*-epimers and  $\sim 4.81\text{ppm}$  for the *R*-epimers.



Proton#	<i>R</i> -epimer reported <sup>[5]</sup>	<i>S</i> -epimer reported <sup>[5]</sup>	<i>R</i> -P1 from SFC	<i>S</i> -P1 from SFC
$\text{C}^1\text{-H}$	7.26 (d, $J_{1,2} = 10.1$ )	7.23 (d, $J_{1,2} = 10.1$ )	7.26 (d, $J_{1,2} = 10.1$ )	7.26 (d, $J_{1,2} = 10.0$ )
$\text{C}^2\text{-H}$	6.27 (dd, $J_{1,2} = 10.1$ , $J_{2,4} = 1.8$ )	6.27 (dd, $J_{1,2} = 10.1$ , $J_{2,4} = 1.8$ )	6.28 (dd, $J_{1,2} = 10.1$ , $J_{2,4} = 1.7$ )	6.27 (dd, $J_{1,2} = 10.1$ , $J_{2,4} = 1.7$ )
$\text{C}^4\text{-H}$	6.03 (m)	6.02 (m)	6.03 (s)	6.02 (s)
$\text{C}^6\text{-H}_2$			2.6-2.53 (m, 1H); 2.37-2.33 (m, 1H)	2.58-2.54 (m, 1H); 2.37-2.33 (m, 1H)
$\text{C}^7\text{-H}_2$			2.10-2.0 (m, 1H); 1.20-1.18 (m, 1H)	2.14-2.0 (m, 1H); 1.19-1.12 (m, 1H)
$\text{C}^8\text{-H}$			2.20-2.18 (m, 1H)	2.14 (m, 1H)
$\text{C}^9\text{-H}$			1.15-1.10 (m, 1H)	1.19-1.12 (m, 1H)
$\text{C}^{11}\text{-H}$	4.4-4.6 (m)	4.50 (m)	4.42-4.60 (m)	4.50 (br s)

C <sup>12</sup> -H <sub>2</sub>			2.09-2.03 (m, 1H), 1.68-1.65 (m, 1H)	2.14-2.04 (m, 1H), 1.67-1.63 (m, 1H)
C <sup>14</sup> -H			1.64-1.63 (m, 1H)	1.87-1.74 (m, 1H)
C <sup>15</sup> -H <sub>2</sub>			1.80-1.75 (m, 1H), 1.63-1.61 (m, 1H)	1.87-1.74 (m, 1H), 1.53-1.48 (m, 1H)
C <sup>16</sup> -H	4.90 (dd, $J_{16\beta\text{H}-15\beta\text{H}} = 4.2$ Hz)	5.16 (dd, $J_{16\beta\text{H}-15\beta\text{H}} = 5.0$ Hz, $J_{16\beta\text{H}-15\alpha\text{H}} = 2.5$ Hz)	4.90 (d, $J_{16\beta\text{H}-15\beta\text{H}} = 4.4$ Hz)	5.19-5.15 (m, 1H)
C <sup>18</sup> -H <sub>3</sub>	0.92 (s)	0.99 (s)	0.92 (s, 3H)	0.99 (s, 3H)
C <sup>19</sup> -H <sub>3</sub>	1.45 (s)	1.45 (s)	1.44 (s, 3H)	1.46 (s, 3H)
C <sup>21</sup> -H <sub>2</sub>	4.50 (dd), 4.25 (dd, $J_{21\text{H}, \text{H}'} = 20.2$ Hz, $J_{21\text{H}-21\text{OH}} = 4.8$ Hz)	4.60 (dd), 4.20 (dd, $J_{21\text{H}, \text{H}'} = 20.2$ Hz, $J_{21\text{H}-21\text{OH}} = 4.8$ Hz)	4.50 (m, 1H); 4.26 (dd, $J_{21\text{H}, \text{H}'} = 20.1$ Hz, $J_{21\text{H}-21\text{OH}} = 4.3$ Hz, 1H))	4.62 (d, $J = 20$ Hz, 1H); 4.21 (d, $J_{21\text{H}, \text{H}'} = 20$ Hz, 1H)
C <sup>22</sup> -H	4.55 (t, $J_{22,23} = 4.2$ Hz)	5.16 (t, $J_{22,23} = 4.6$ Hz)	4.55 (t, $J = 4.6$ Hz)	5.19-5.15 (m, 1H)
C <sup>23</sup> -H <sub>2</sub>			1.64-1.61 (m, 2H)	1.59-1.54 (m, 2H)
C <sup>24</sup> -H <sub>2</sub>			1.41-1.35 (m, 2H)	1.40-1.29 (m, 2H)
C <sup>25</sup> -H <sub>3</sub>	0.92 (t, $J_{24,25} = 6.7$ Hz)	0.91 (t, $J_{24,25} = 7.3$ Hz)	0.92 (t, $J_{24,25} = 7.3$ Hz)	0.91 (t, $J_{24,25} = 7.3$ Hz)

**Table S2.** Comparison of <sup>1</sup>H NMR chemical shifts (ppm in CDCl<sub>3</sub>) of reported *R*-/*S*-Budesonide epimers and *R*-**P1** and *S*-**P1** isolated from SFC.

3D-model structures for the *R*-**P3** and *S*-**P3** epimers are shown in Figure S8. Based on these conformational models, there is a steric repulsion between the C<sup>22</sup>-proton and C<sup>16</sup>-proton in the *R*-epimer, but not in the *S*-epimer. Simultaneously, the C<sup>22</sup>-proton in the *R*-epimer is shielded by an

anisotropy effect from the C<sup>20</sup>-carbonyl group, but not in the *S*-epimer. This is consistent with the <sup>1</sup>H NMR spectra where both the C<sup>22</sup>-proton and C<sup>16</sup>-proton in the *S*-epimers are observed to be deshielded as compared to the corresponding protons in the *R*-epimers (Table S3). Taken together, these findings suggest that the conformations of the dioxolane ring in both *S*- and *R*-epimers are not same.

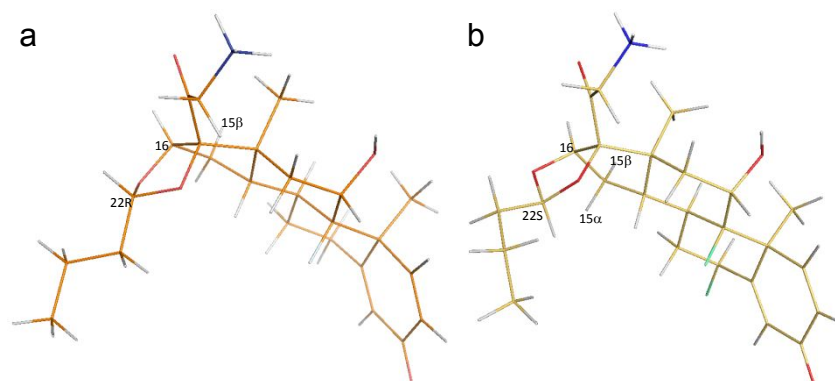
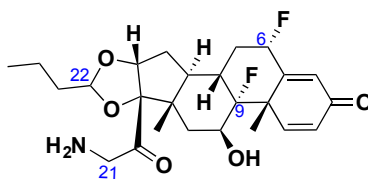


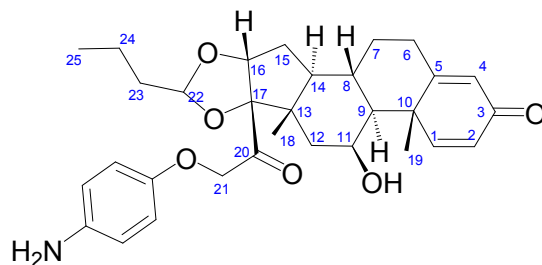
**Figure S8. Models of 3D-structure of *R*-P3 (a) and *S*-P3 (b)**



Proton #	<i>R</i> -P3	<i>S</i> -P3
N-H <sub>3</sub>	8.14 (s, 3H)	8.12 (brs, 3H),
C <sup>1</sup> -H	7.30 (d, <i>J</i> = 10.0 Hz, 1H)	7.30 (d, <i>J</i> = 10.0 Hz, 1H),
C <sup>2</sup> -H	6.31 (dd, <i>J</i> = 10.0 Hz, 1.6 Hz, 1H)	6.30 (dd, <i>J</i> = 1.6 Hz, 10.0 Hz, 1H),
C <sup>4</sup> -H	6.11 (s, 1H)	6.11 (s, 1H),
C <sup>6</sup> -H	5.71-5.55 (m, 1H)	5.71-5.54 (m, 1H),
C <sup>7</sup> -H <sub>2</sub>	2.28-2.26 (m, 1H); 1.68-1.56 (m, 1H)	2.25-2.22 (m, 1H); 1.72-1.52 (m, 1H)
C <sup>8</sup> -H	1.44-1.31 (m, 1H)	1.87-1.79 (m, 1H)
C <sup>11</sup> -H	4.22 (m, 1H)	4.18 (m, 1H)

C <sup>12</sup> -H <sub>2</sub>	2.09-2.01 (m, 1H), 1.68-1.56 (m, 1H)	2.03-1.97 (m, 1H), 1.72-1.52 (m, 1H)
C <sup>14</sup> -H	2.09-2.01 (m, 1H)	2.03-1.97 (m, 1H)
C <sup>15</sup> -H <sub>2</sub>	2.67-2.50 (m, 1H); 1.68-1.56 (m, 1H)	2.58-2.53 (m, 1H); 1.72-1.52 (m, 1H)
C <sup>16</sup> -H	4.78 (m, 1H)	5.15 (d, <i>J</i> = 7.6 Hz, 1 H)
C <sup>18</sup> -H <sub>3</sub>	0.85 (s, 3H)	0.91 (s, 3H)
C <sup>19</sup> -H <sub>3</sub>	1.48 (s, 3H)	1.48 (s, 3H)
C <sup>21</sup> -H <sub>2</sub>	4.20 (d, <i>J</i> = 19 Hz, 1H); 3.77 (d, <i>J</i> = 19 Hz, 1H)	4.15 (d, <i>J</i> = 19 Hz, 1H); 3.74 (d, <i>J</i> = 19 Hz, 1H)
C <sup>22</sup> -H	4.67 (t, <i>J</i> = 4.4 Hz, 1H)	5.22 (t, <i>J</i> = 4.8 Hz, 1H)
C <sup>23</sup> -H <sub>2</sub>	1.68-1.56 (m, 2H)	1.48 (m, 2H)
C <sup>24</sup> -H <sub>2</sub>	1.44-1.31 (m, 2H)	1.34-1.28 (m, 1H)
C <sup>25</sup> -H <sub>3</sub>	0.87 (t, <i>J</i> = 7.2 Hz, 3H)	0.88 (t, <i>J</i> = 7.6 Hz, 3 H)

**Table S3.** Comparison of <sup>1</sup>H NMR chemical shifts (ppm in *d*<sub>6</sub>-DMSO) of *R*-**P3** and *S*-**P3** isolated from SFC.

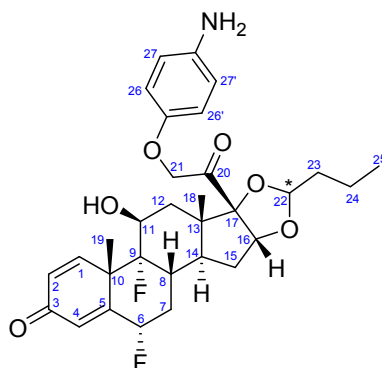


Proton #	<b>S-P10</b>	<b>R-P10</b>
C <sup>1</sup> -H	7.21, 1H (d, <i>J</i> = 10.1 Hz)	7.23, 1H (d, <i>J</i> = 10.1 Hz)
C <sup>2</sup> -H	6.24, 1H (dd, <i>J</i> = 10.1 Hz, 1.6 Hz)	6.27, 1H (dd, <i>J</i> = 10.1 Hz, 1.6 Hz)
C <sup>4</sup> -H	6.02, 1H (s)	6.04, 1H (s)

C <sup>6</sup> -H	2.57, 1H (td, $J = 13.2$ Hz, 4.4 Hz); 2.34, 1H (td, $J = 13.4$ Hz, 3.2 Hz)	2.58, 1H (td, $J = 13.3$ Hz, 4.9 Hz); 2.35, 1H (td, $J = 13.4$ Hz, 2.8 Hz)
C <sup>7</sup> -H <sub>2</sub>	2.16-2.01, 1H (m); 1.18-1.09, 1H (m)	2.23-1.99, 1H (m); 1.23-1.09, 1H (m)
C <sup>8</sup> -H	2.16-2.01, 1H (m)	2.23-1.99, 1H (m)
C <sup>9</sup> -H	1.18-1.09, 1H (m)	1.23-1.09, 1H (m)
C <sup>11</sup> -H	4.43, 1H (s)	4.48, 1H (d, $J = 2.1$ Hz)
C <sup>12</sup> -H <sub>2</sub>	2.16-2.01, 1H (m); 1.59-1.49, 1H (m)	2.23-1.99, 1H (m); 1.79-1.61, 1H (m)
C <sup>14</sup> -H	1.59-1.49, 1H (m)	1.79-1.61, 1H (m)
C <sup>15</sup> -H <sub>2</sub>	1.59-1.49, 2H (m)	1.79-1.61, 2H (m)
C <sup>16</sup> -H	5.20, 1H (d, $J = 6.8$ Hz)	4.94, 1H (d, $J = 4.4$ Hz)
C <sup>18</sup> -H <sub>3</sub>	1.00, 3H (s)	0.95, 3H (s)
C <sup>19</sup> -H <sub>3</sub>	1.44, 3H (s)	1.44, 3H (s)
C <sup>21</sup> -H <sub>2</sub>	4.99; 4.61, 2H (d, $J = 18.0$ Hz)	4.65; 4.89, 2H (dd, $J = 18.0$ Hz, $J = 4.4$ Hz)
C <sup>22</sup> -H	5.18, 1H (t, $J = 4.8$ Hz)	4.61, 1H (t, $J = 4.4$ Hz)
C <sup>23</sup> -H <sub>2</sub>	1.59-1.49, 2H (m)	1.79-1.61, 2H (m)
C <sup>24</sup> -H <sub>2</sub>	1.44-1.26, 2H (m)	1.46-1.38, 2H (m)
C <sup>25</sup> -H <sub>3</sub>	0.91, 3H (t, $J = 7.3$ Hz)	0.93, 3H (t, $J = 7.3$ Hz)
26	6.77, 2H (d, $J = 8.8$ Hz)	6.79, 2H (d, $J = 8.8$ Hz)

27	6.63, 2H (d, $J = 8.8$ Hz)	6.65, 2H (d, $J = 8.8$ Hz)
----	----------------------------	----------------------------

**Table S4.** Comparison of  $^1\text{H}$  NMR chemical shifts (ppm in  $\text{CDCl}_3$ ) of *R*-**P10** and *S*-**P10** isolated from SFC.



Proton #	<i>R</i> - <b>P12</b>	<i>S</i> - <b>P12</b>
-NH <sub>2</sub>	4.71-4.67 (m, 2H)	4.69 (s, 2H)
C <sup>1</sup> -H	7.26 (d, $J = 10.1$ Hz, 1H)	7.27 (dd, $J = 10.2, 1.0$ Hz, 1H)
C <sup>2';6'</sup> -H <sub>2</sub>	6.64 (d, $J = 8.8$ Hz, 2H)	6.65-6.60 (m, 2H)
C <sup>3';5'</sup> -H <sub>2</sub>	6.50 (d, $J = 8.8$ Hz, 2H)	6.51-6.47 (m, 2H)
C <sup>2</sup> -H	6.30 (dd, $J = 10.1$ Hz, 1.8 Hz, 1H)	6.30 (dd, $J = 10.2, 1.9$ Hz, 1H)
C <sup>4</sup> -H	6.11 (s, 1H)	6.11 (s, 1H)
C <sup>6</sup> -H	5.72-5.55 (m, 1H)	5.71-5.67 (m, 1H)
-OH	5.51(d, $J = 2.2$ Hz, 1H)	5.52 (t, $J = 4.9$ Hz, 1H)
C <sup>7</sup> -H <sub>2</sub>	2.28-2.25 (m, 1H); 1.60-1.52 (m, 1H)	2.26-2.23 (m, 1H); 1.65-1.52 (m, 1H)
C <sup>8</sup> -H	1.45-1.41 (m, 1H)	1.49-1.41 (m, 1H)
C <sup>11</sup> -H	4.21 (m, 1H)	4.19 (m, 1H)
C <sup>12</sup> -H <sub>2</sub>	2.10-2.01 (m, 1H), 1.77 (d, $J = 13$ Hz, 1H)	2.09-2.01 (m, 1H), 1.84-1.76 (m, 1H)
C <sup>14</sup> -H	2.10-2.01 (m, 1H)	2.09-2.01 (m, 1H)
C <sup>15</sup> -H <sub>2</sub>	2.67-2.60 (m, 1H), 1.60-1.52 (m, 1H)	2.60-2.51 (m, 1H), 1.65-1.56 (m, 1H)



C <sup>16</sup> -H	4.71-4.67 (m, 1H)	5.15 (d, <i>J</i> = 7.2 Hz, 1H)
C <sup>18</sup> -H <sub>3</sub>	0.83 (s, 3H)	0.92-0.78 (m, 3H)
C <sup>19</sup> -H <sub>3</sub>	1.49 (s, 3H)	1.49 (s, 3H)
C <sup>21</sup> -H <sub>2</sub>	4.97 (d, <i>J</i> = 18.4 Hz, 1H); 4.71-4.67 (m, 1H)	4.99 (d, <i>J</i> = 18.0 Hz, 1H); 4.63 (d, <i>J</i> = 18.0 Hz, 1H)
C <sup>22</sup> -H	4.79 (m, 1H)	5.23 (t, <i>J</i> = 4.8 Hz, 1H)
C <sup>23</sup> -H <sub>2</sub>	1.60-1.52 (m, 2H)	1.65-1.56 (m, 2H)
C <sup>24</sup> -H <sub>2</sub>	1.39-1.31 (m, 2H)	1.34-1.23 (m, 2H)
C <sup>25</sup> -H <sub>3</sub>	0.87 (t, <i>J</i> = 7.6 Hz, 3H)	0.92-0.78 (m, 3H)

**Table S5.** Comparison of <sup>1</sup>H NMR chemical shifts (ppm in *d*<sub>6</sub>-DMSO) of *R*-**P12** and *S*-**P12** isolated from SFC.

## 2.5 LC-MS of all payloads and linker-payloads

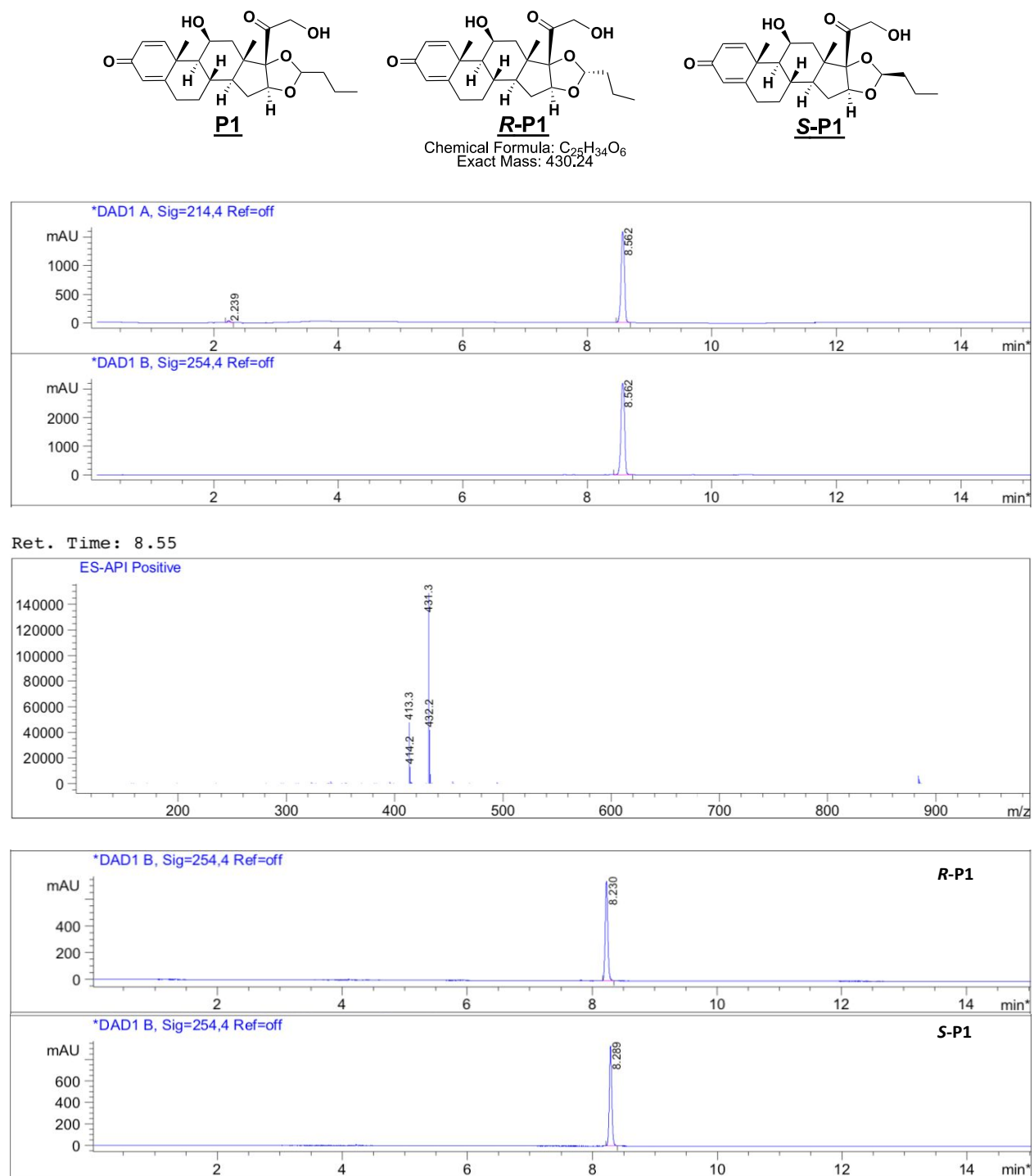


Figure S9. LC-MS of P1, LC of R-P1 and S-P1

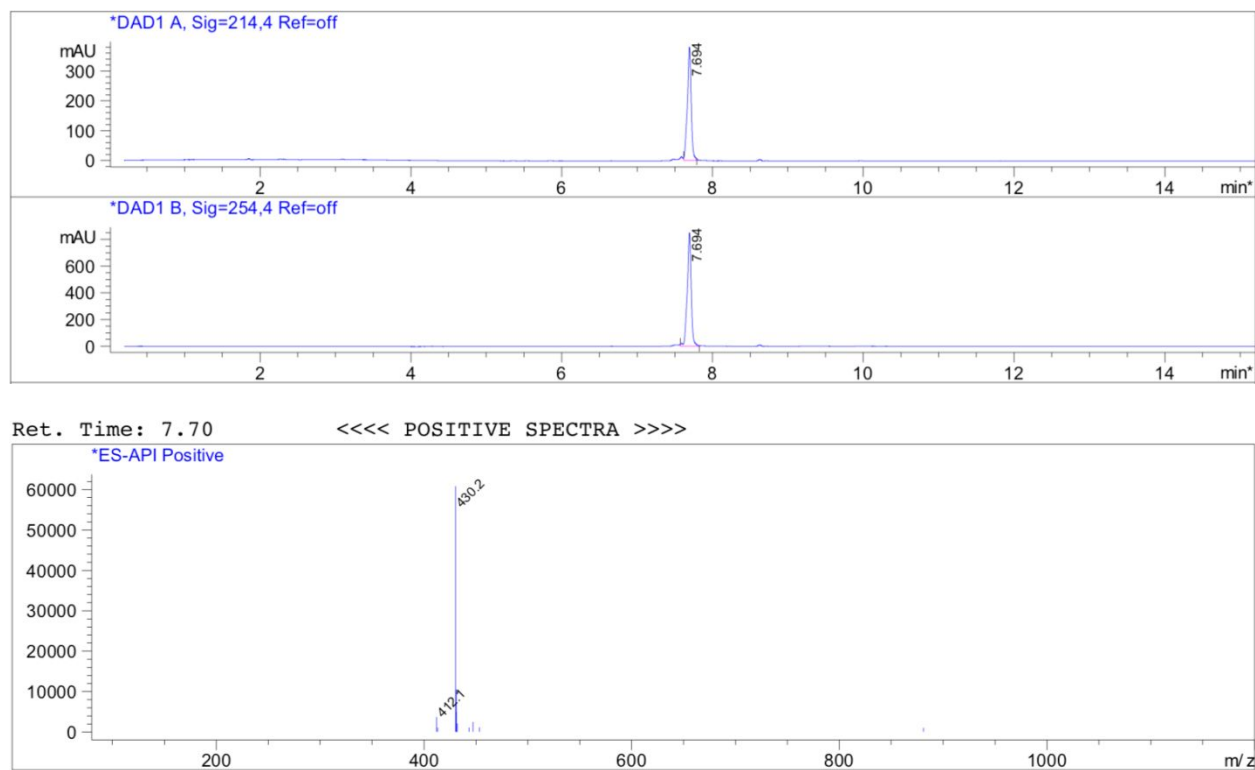
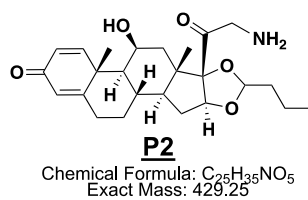
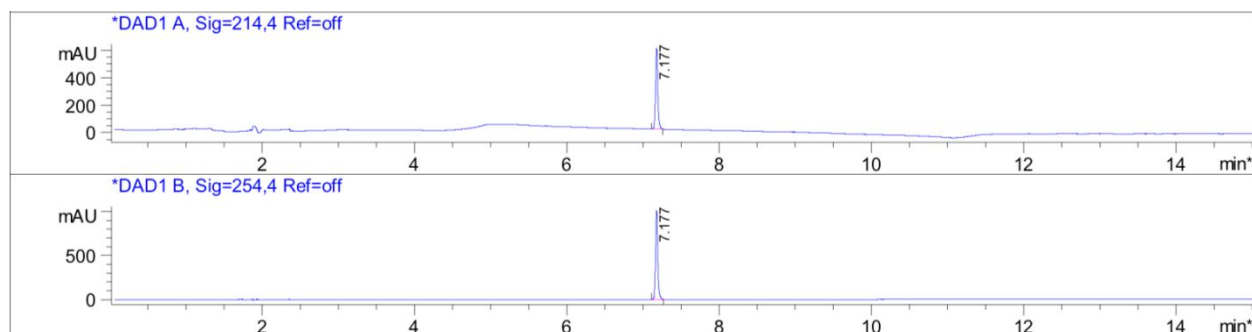
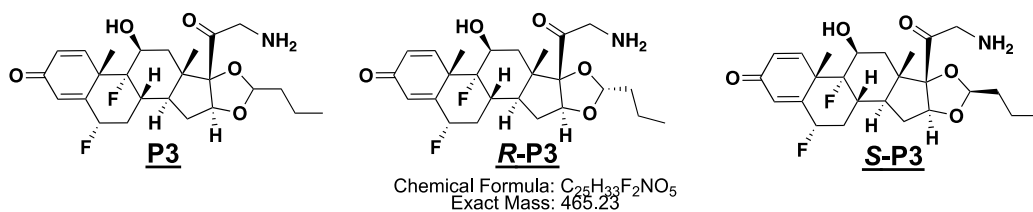


Figure S10. LC-MS of P2



Ret. Time: 7.17

<<<< POSITIVE SPECTRA >>>>

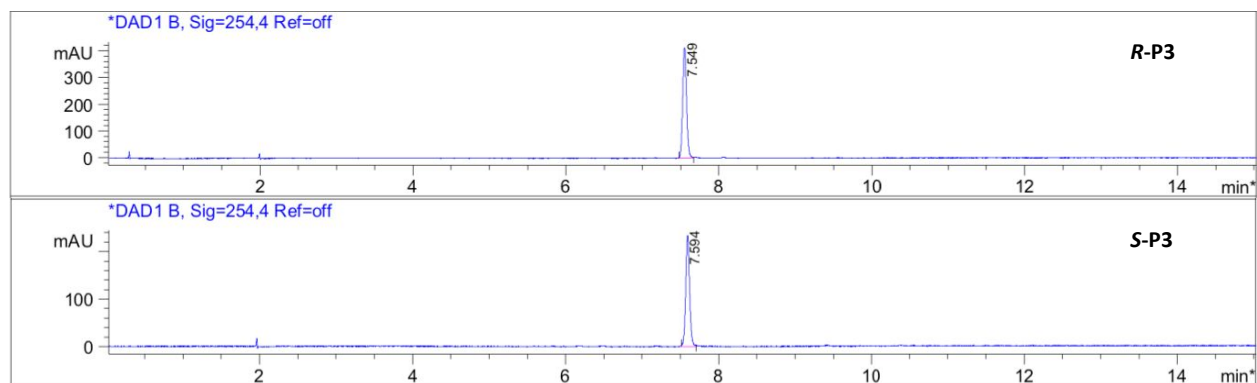
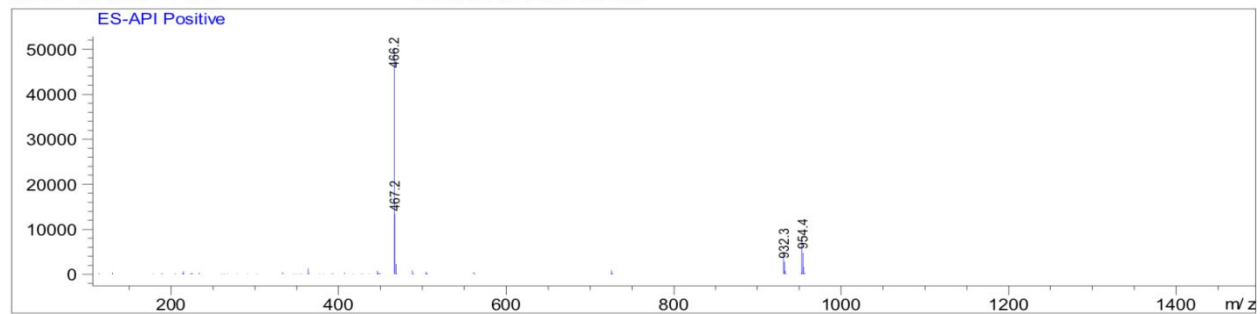
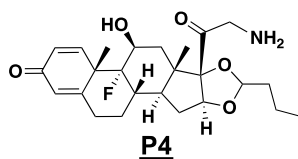
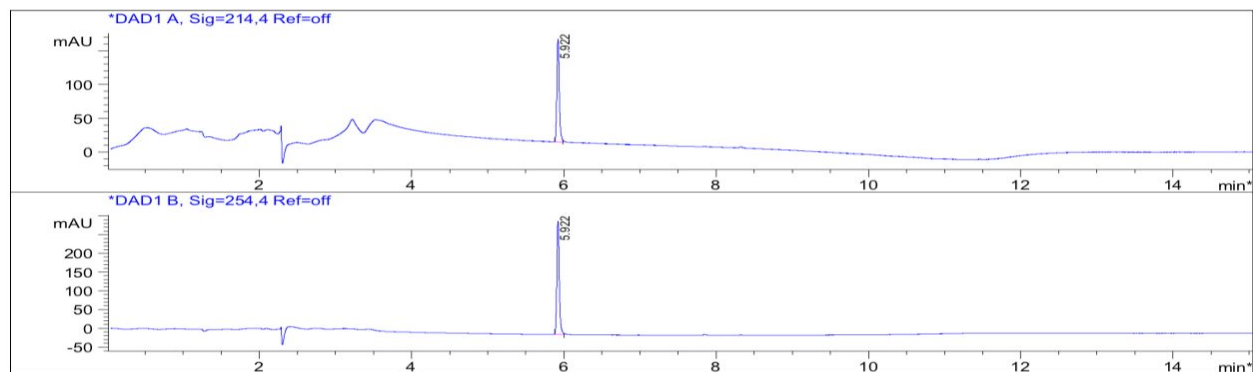


Figure S11. LC-MS of P3, LC of *R*-P3 and *S*-P3



Chemical Formula:  $C_{25}H_{34}FNO_5$   
Exact Mass: 447.24



Ret. Time: 5.95

<<<< POSITIVE SPECTRA >>>>

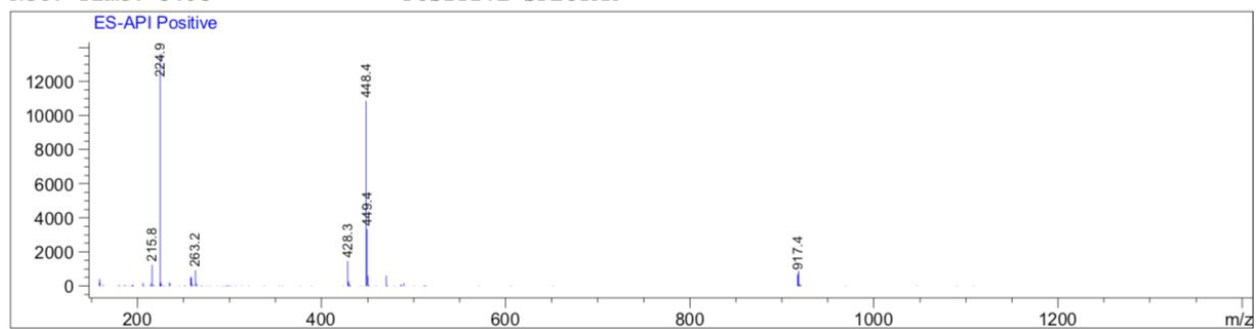


Figure S12. LC-MS of P4

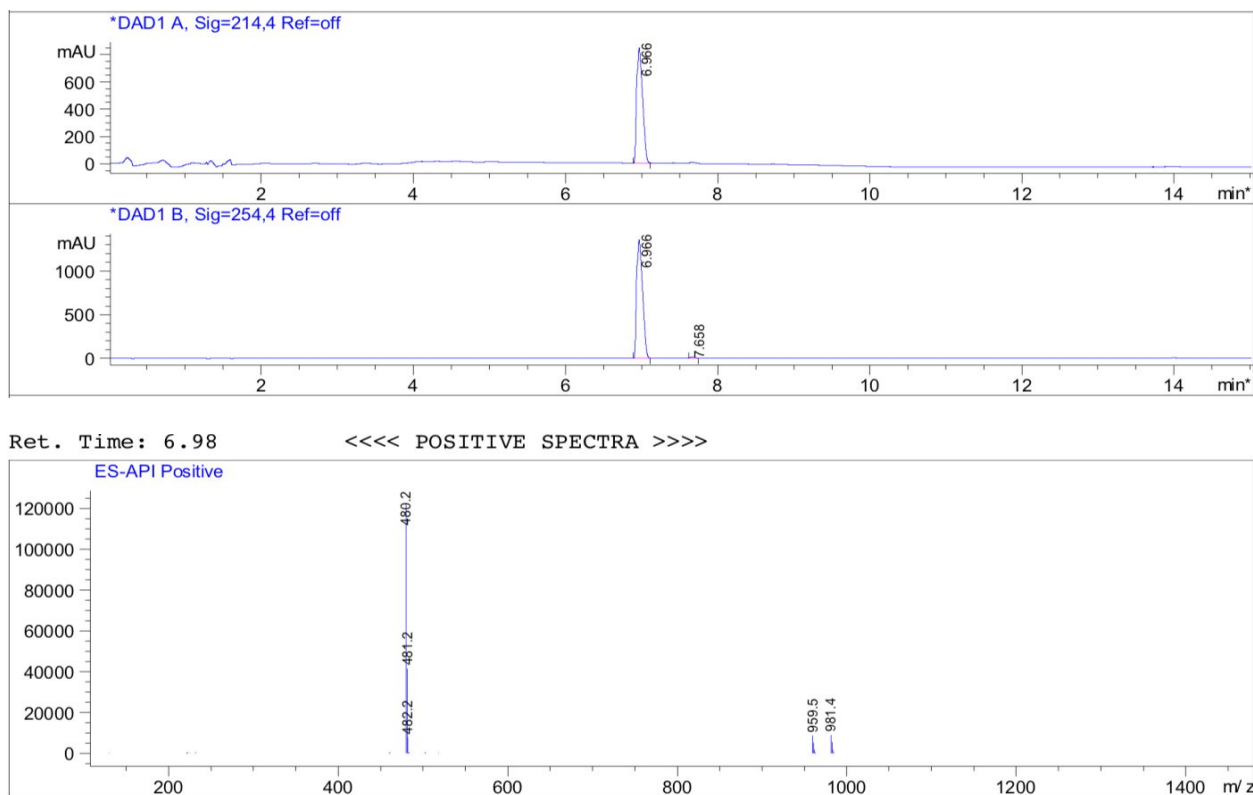
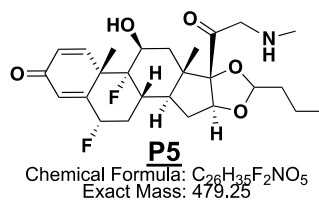


Figure S13. LC-MS of P5

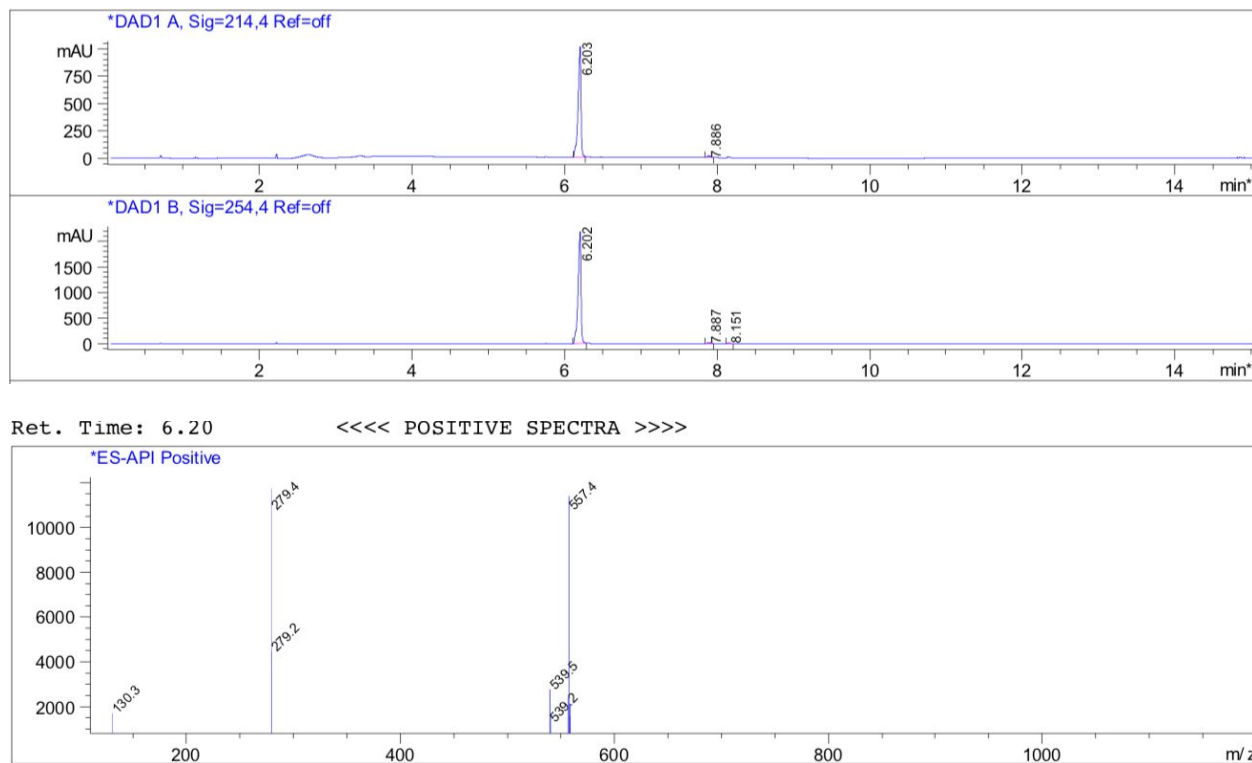
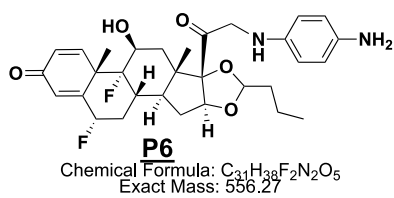
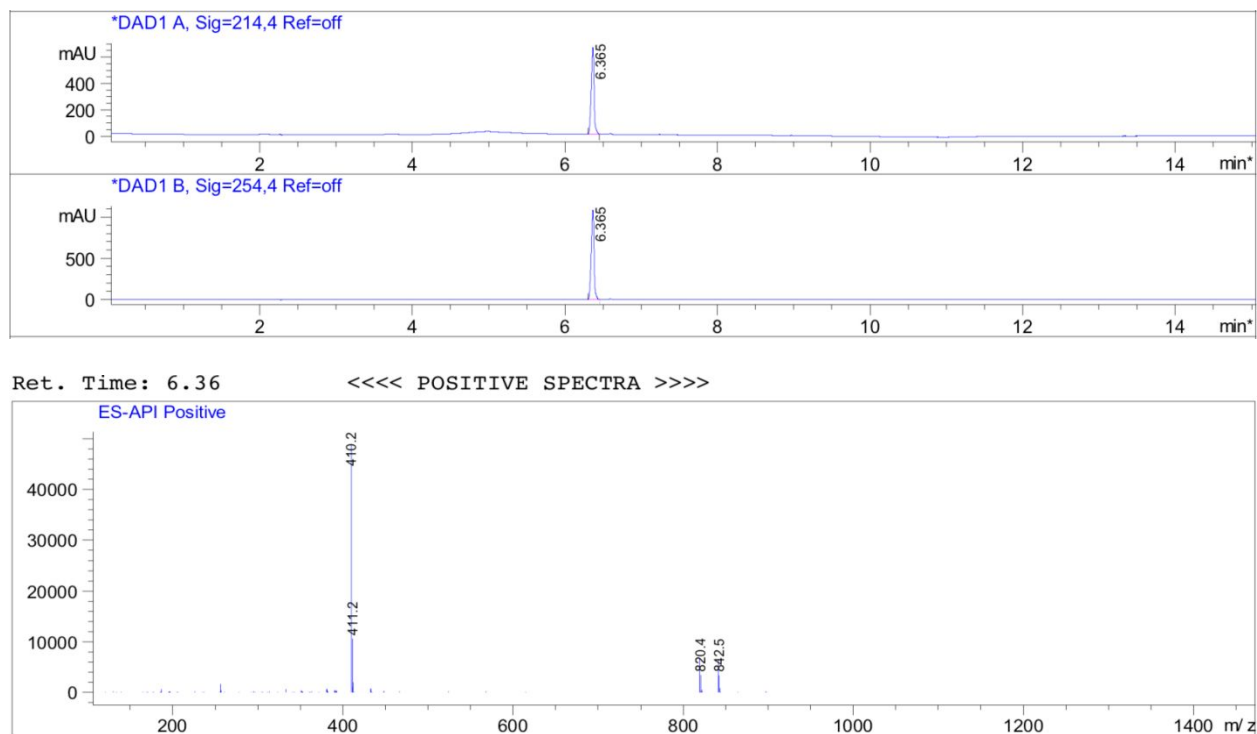
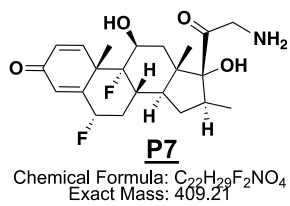
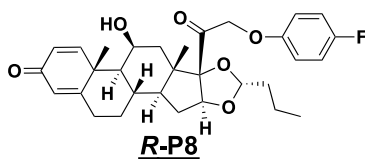


Figure S14. LC-MS of P6

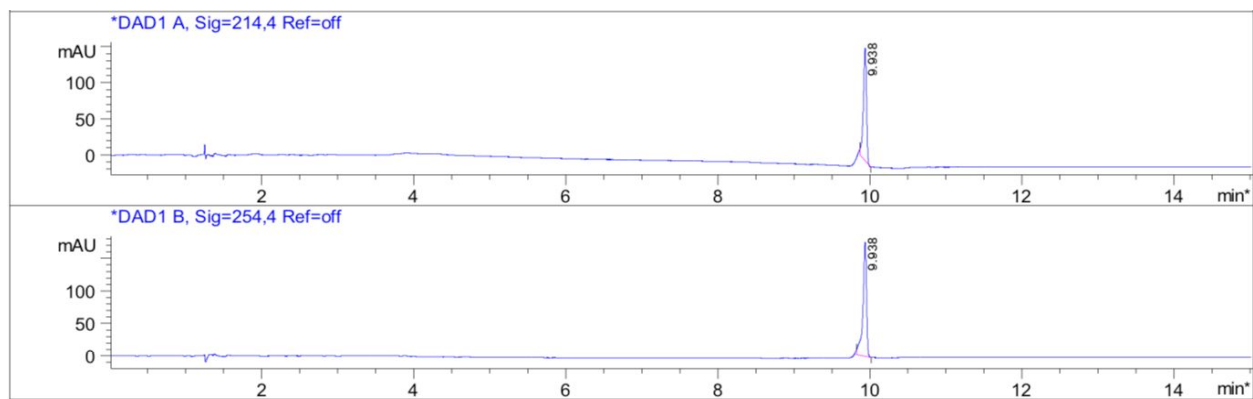


**Figure S15. LC-MS of P7**





Chemical Formula:  $C_{31}H_{37}FO_6$   
Exact Mass: 524.26



Ret. Time: 9.95

<<<< POSITIVE SPECTRA >>>>

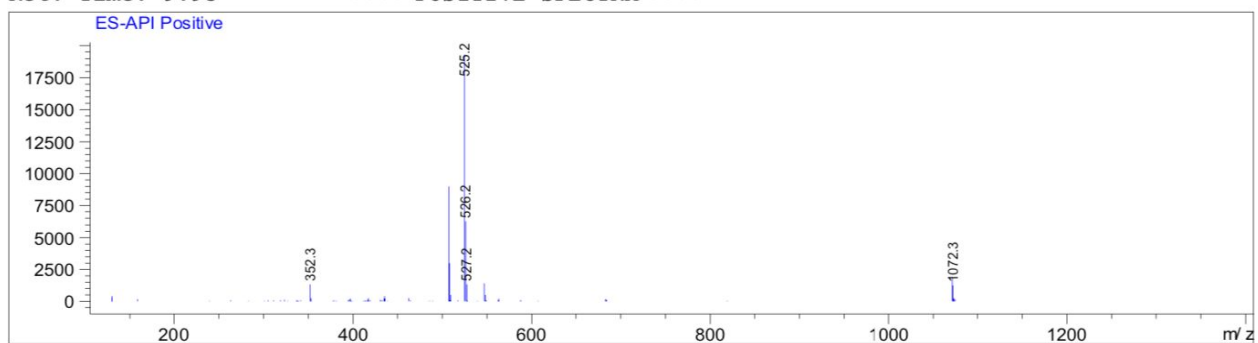
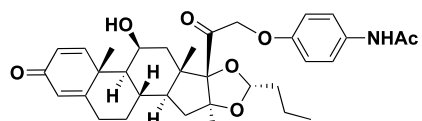
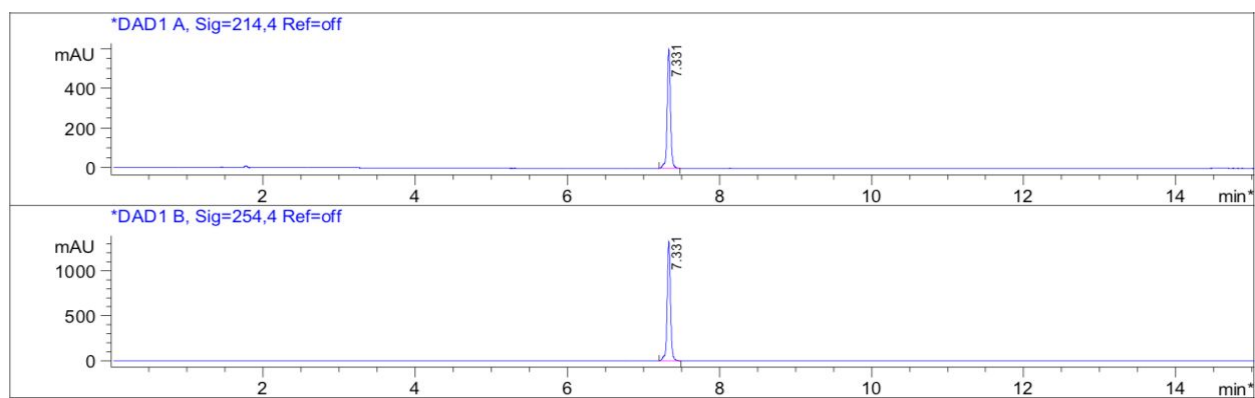


Figure S16. LC-MS of *R-P8*



**R-P9**

Chemical Formula:  $C_{33}H_{41}NO_7$   
Exact Mass: 563.29



Ret. Time: 7.33

<<<< POSITIVE SPECTRA >>>>

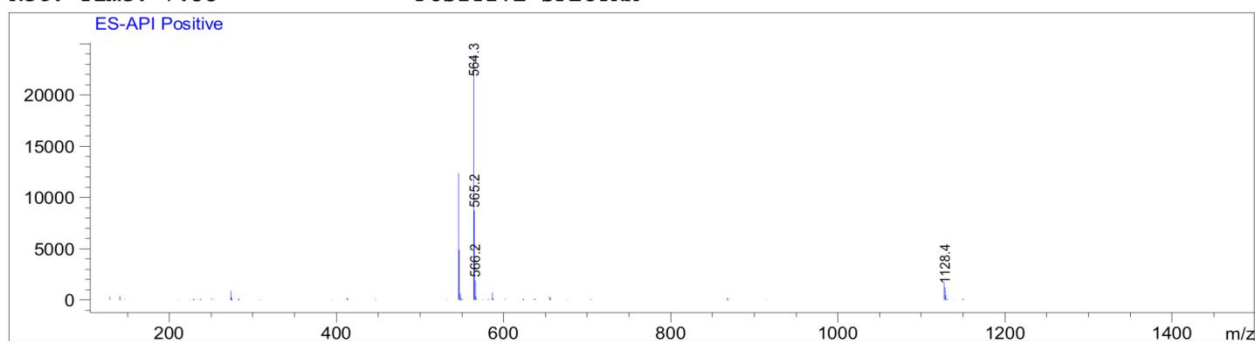


**Figure S17. LC-MS of R-P9**

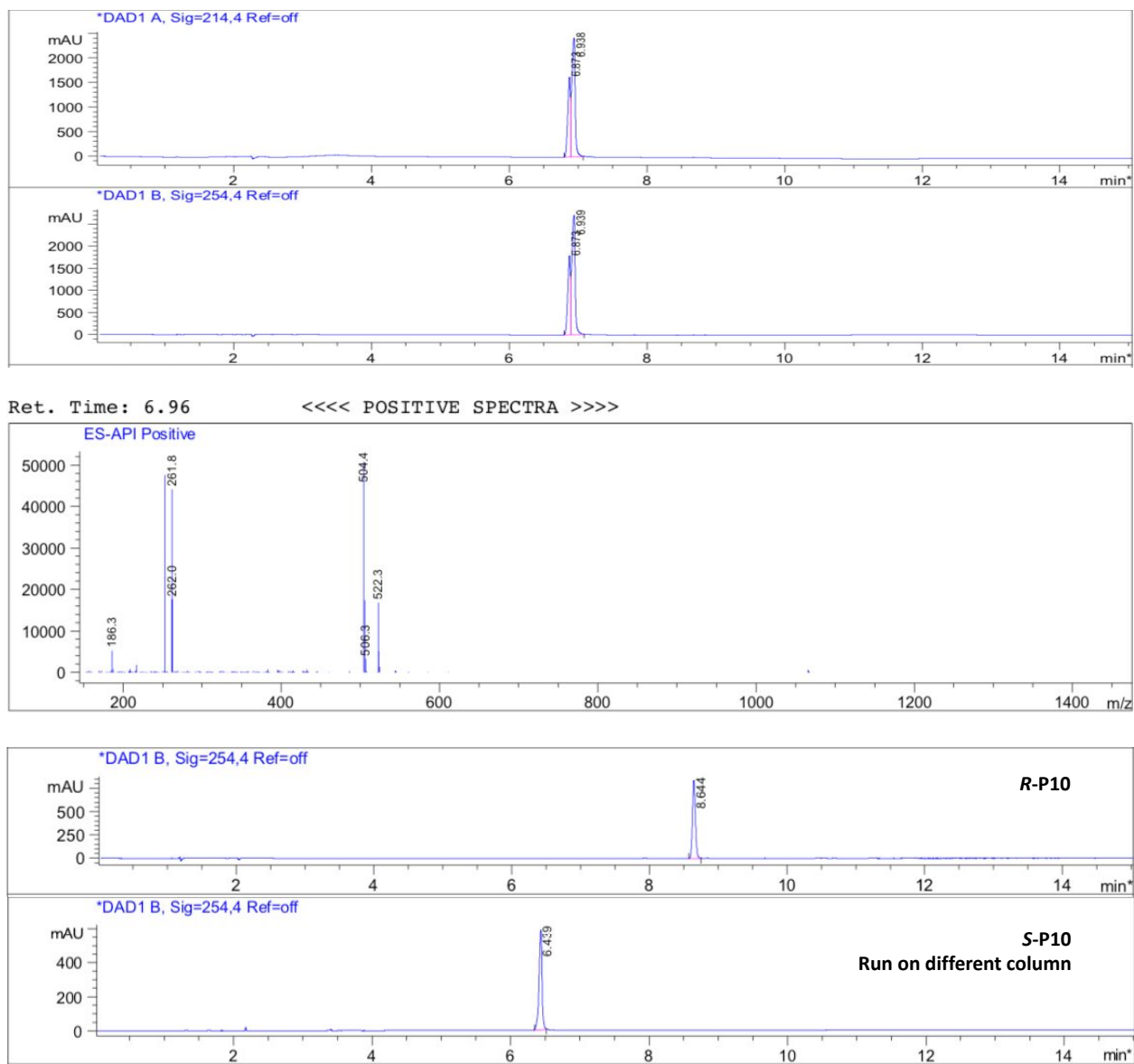
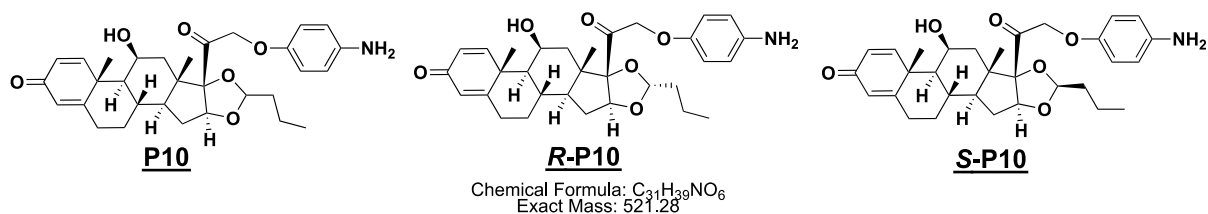
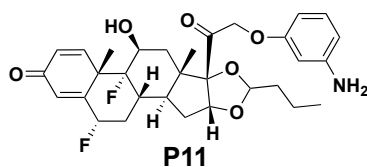
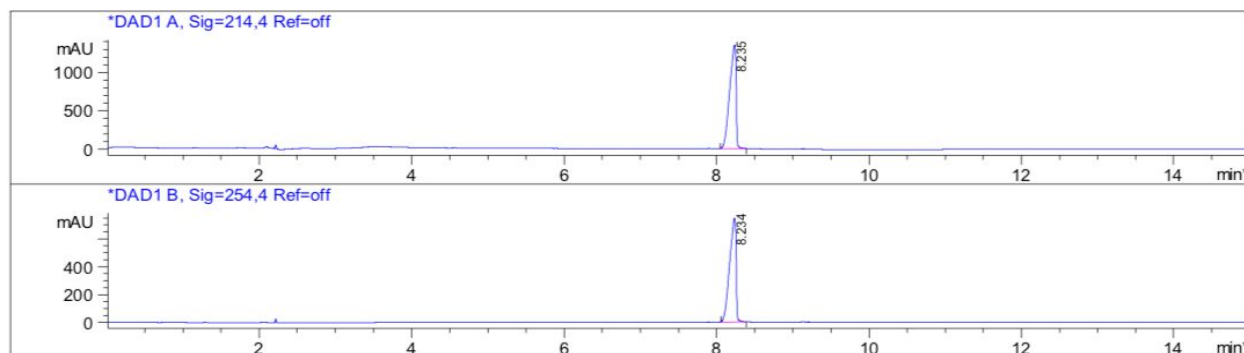


**Figure S18. LC-MS of P10, LC of R-P10 and S-P10**



Chemical Formula:  $C_{31}H_{37}F_2NO_6$   
Exact Mass: 557.26



Ret. Time: 8.25

<<<< POSITIVE SPECTRA >>>>

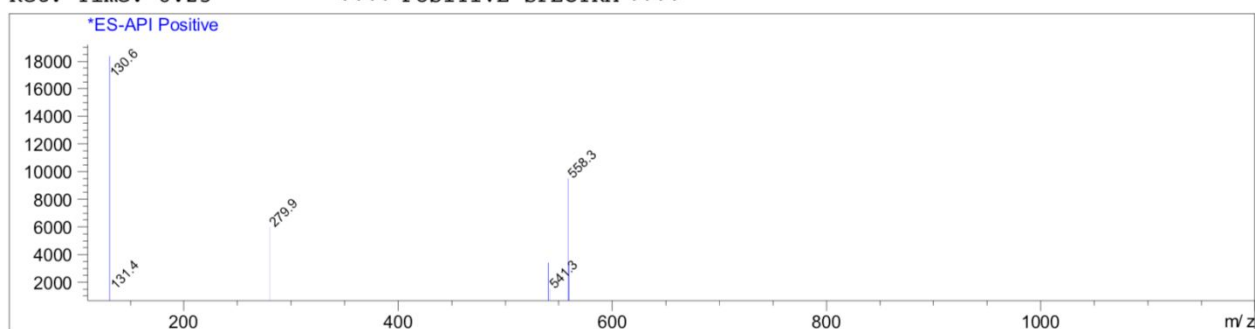
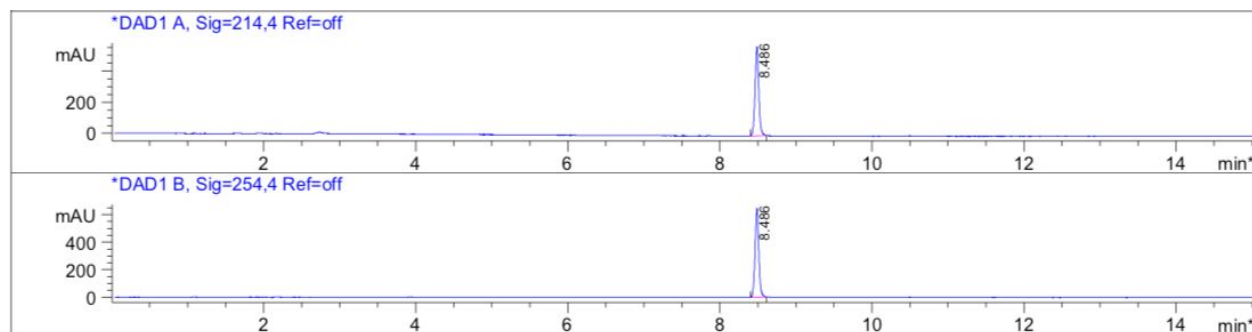
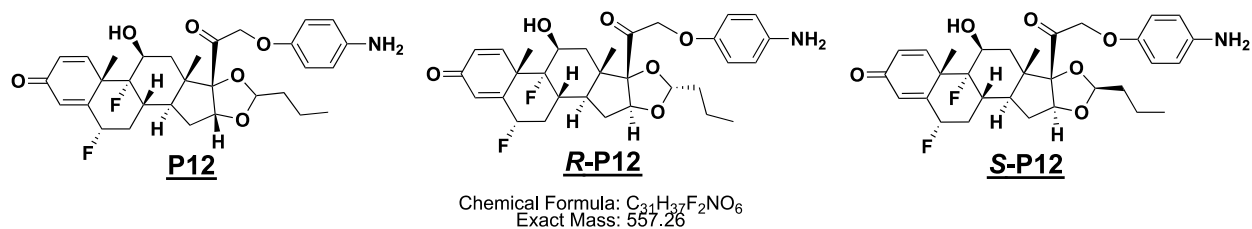


**Figure S19. LC-MS of P11**



Ret. Time: 8.49

<<<< POSITIVE SPECTRA >>>>

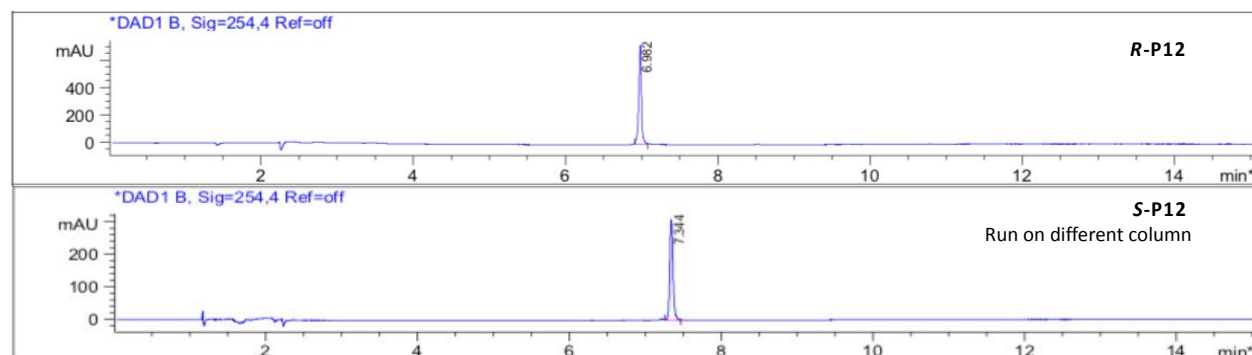
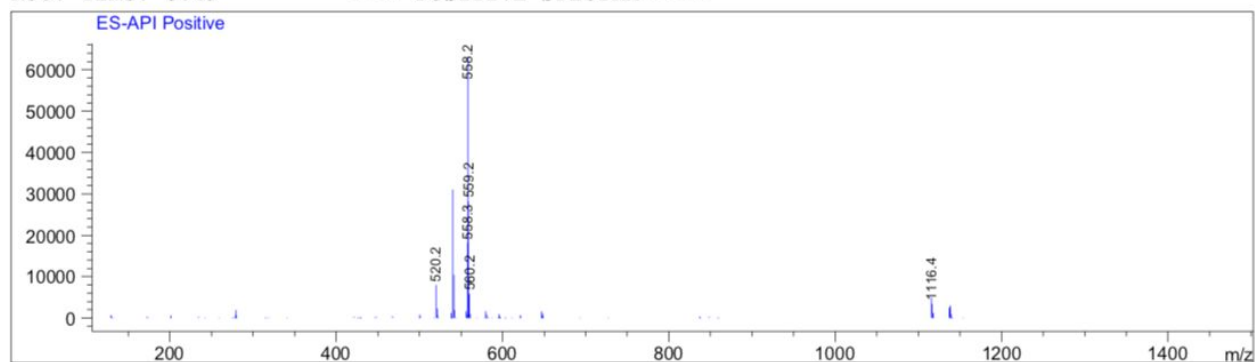
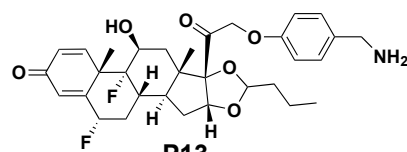
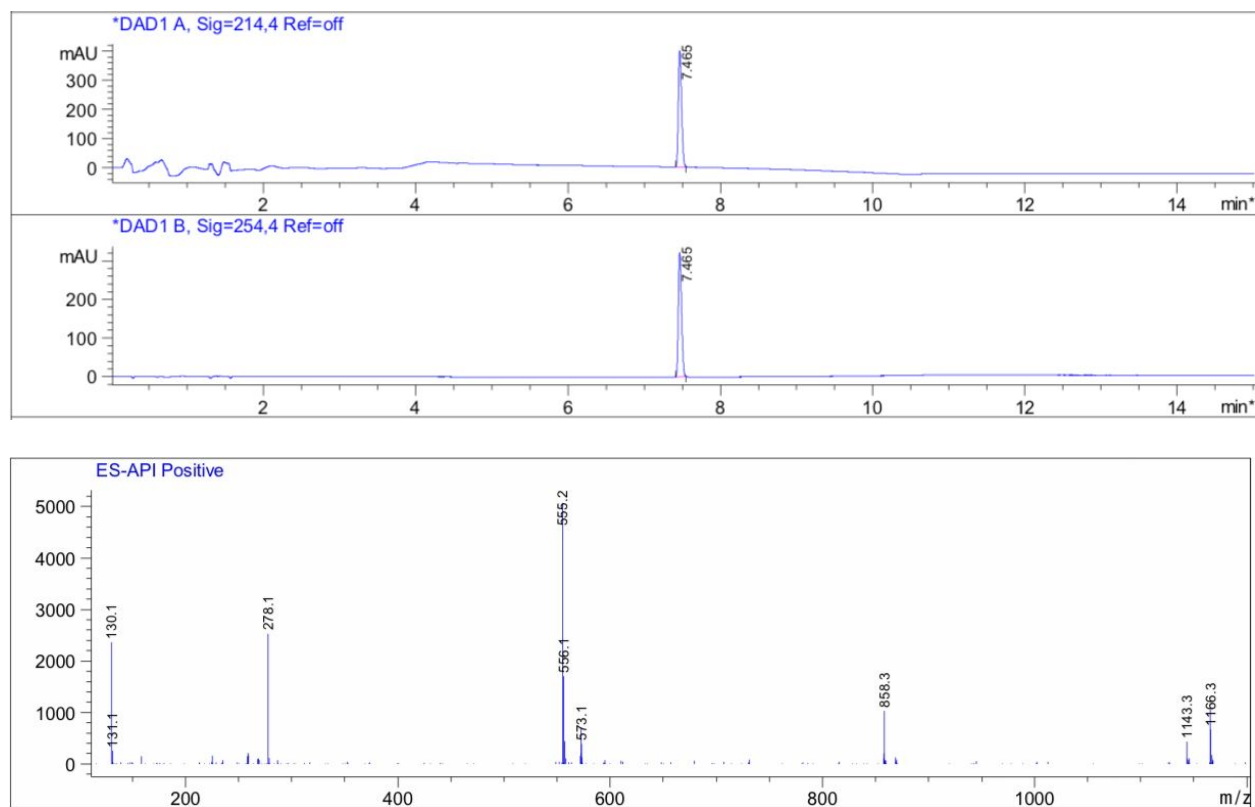


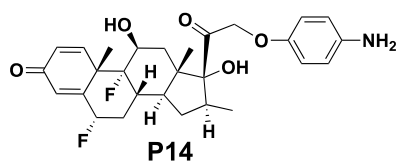
Figure S20. LC-MS of P12, LC of R-P12 and S-P12



Chemical Formula:  $C_{32}H_{39}F_2NO_6$   
 Exact Mass: 571.27



**Figure S21. LC-MS of P13**



Chemical Formula:  $C_{28}H_{32}F_2NO_5$   
 Exact Mass: 501.23

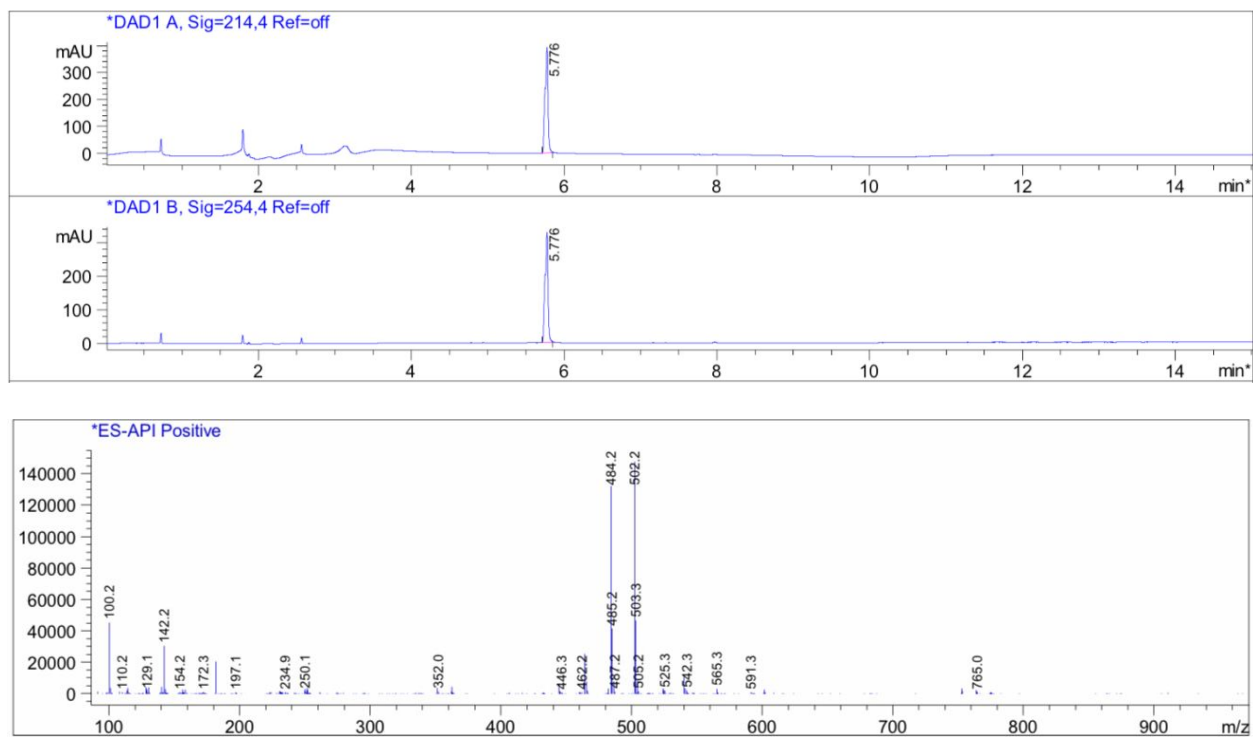
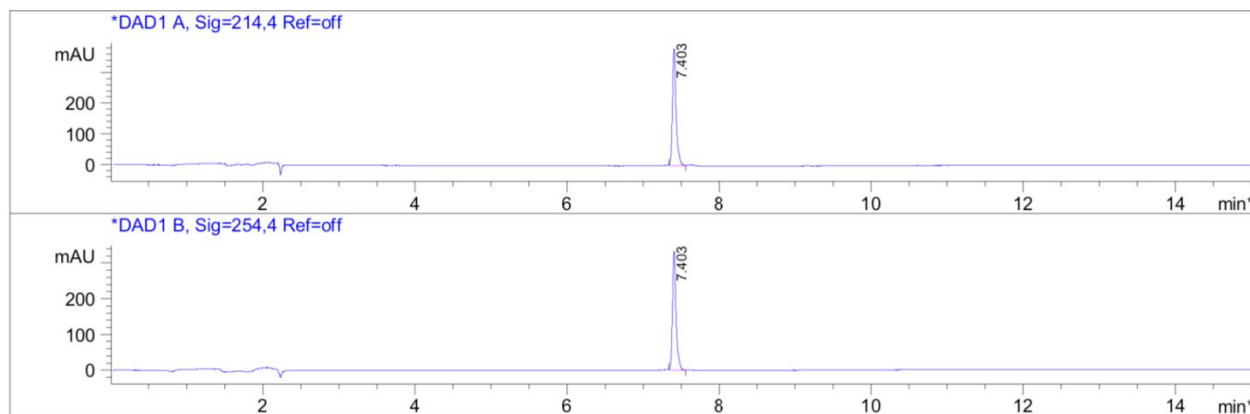
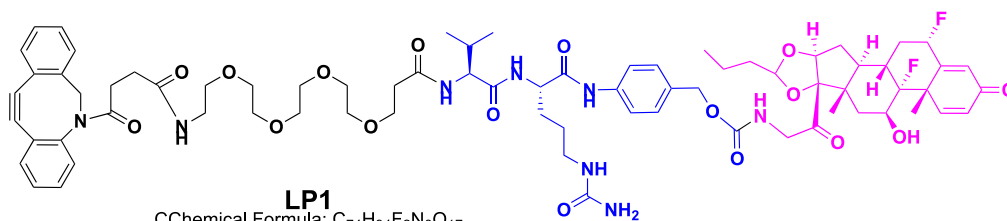


**Figure S22. LC-MS of P14**



Ret. Time: 7.45

<<<< POSITIVE SPECTRA >>>>

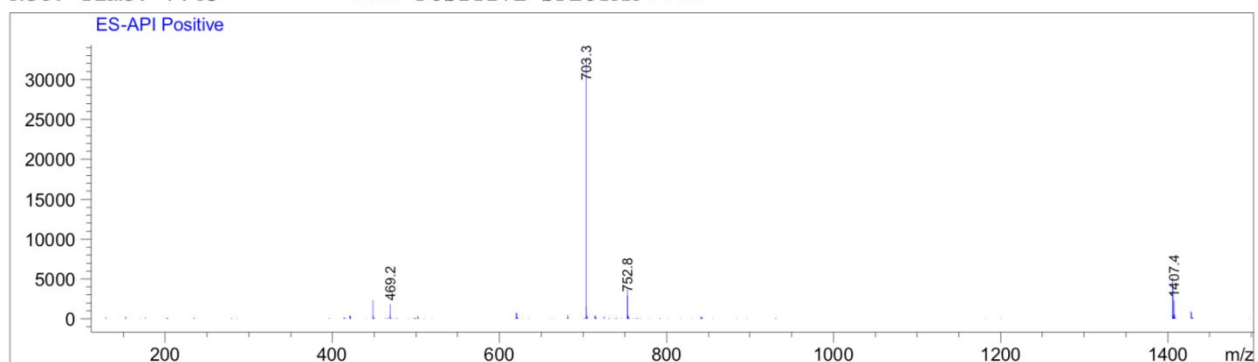
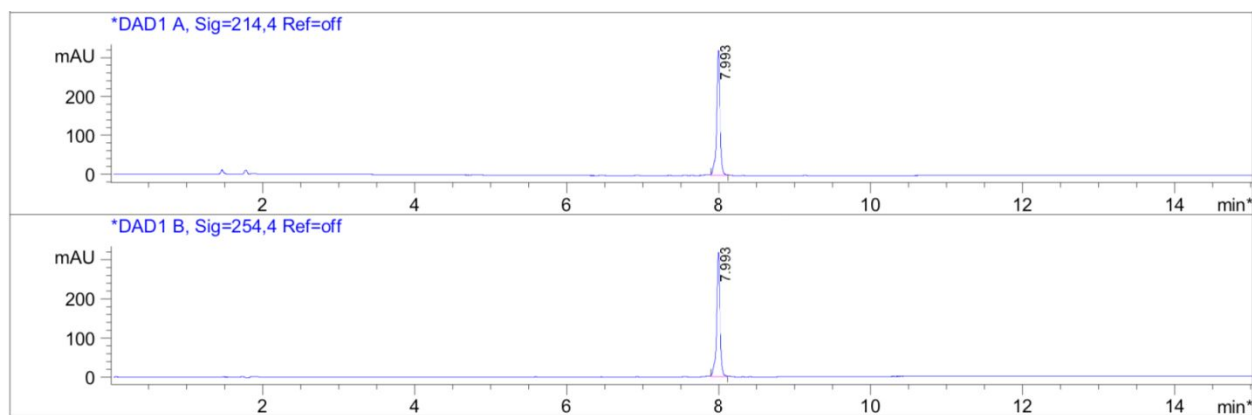
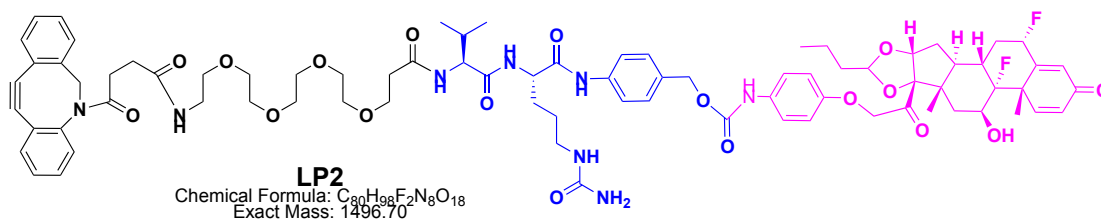


**Figure S23. LC-MS of LP1**





Ret. Time: 7.96

<<<< POSITIVE SPECTRA >>>>

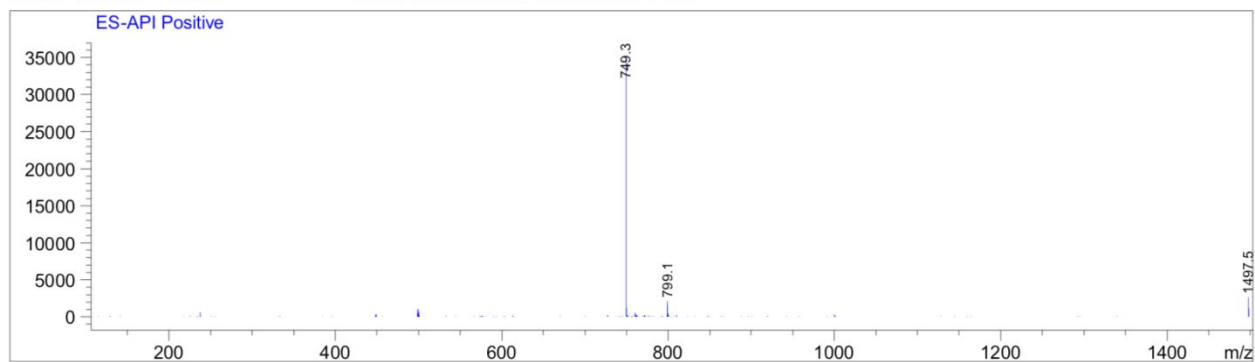
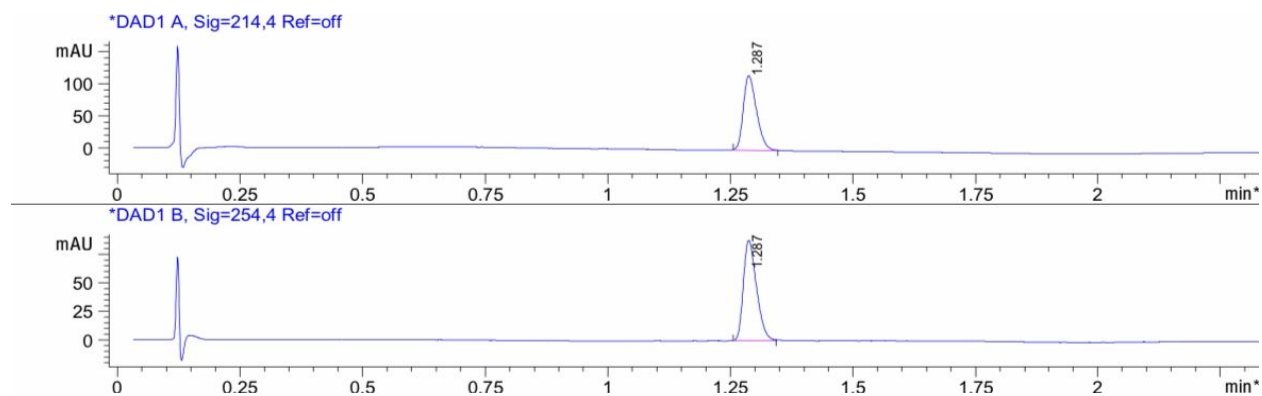
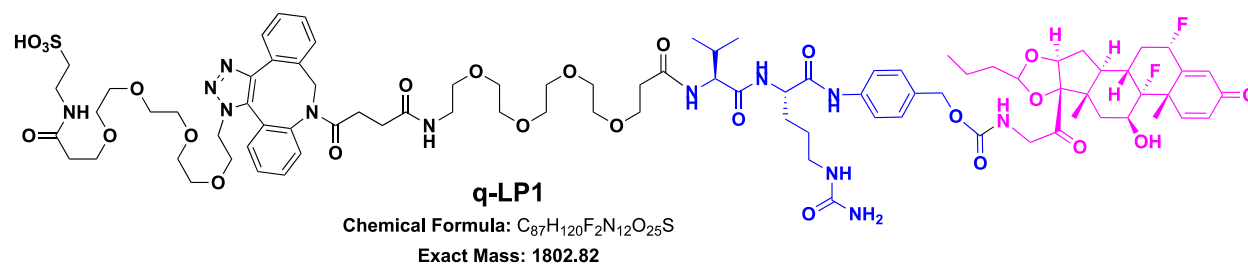


Figure S24. LC-MS of LP2



LC/MS Report

Ret. Time: 1.29

<<<< POSITIVE SPECTRA >>>>

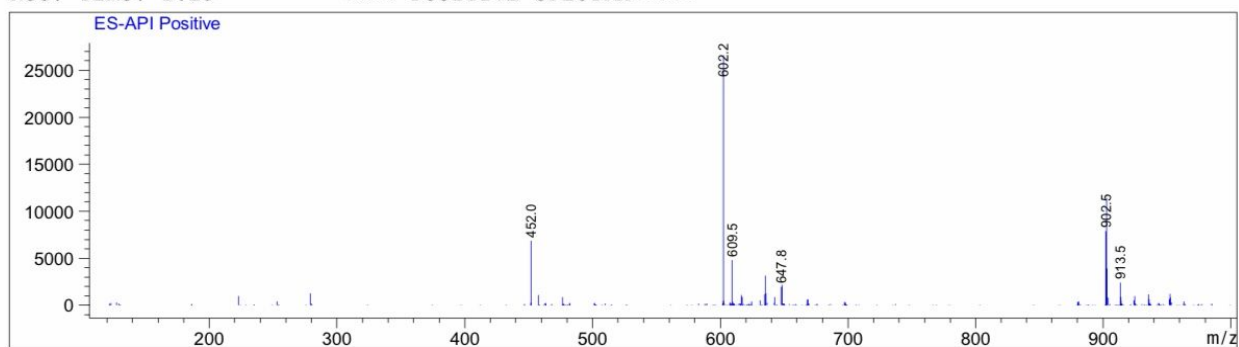
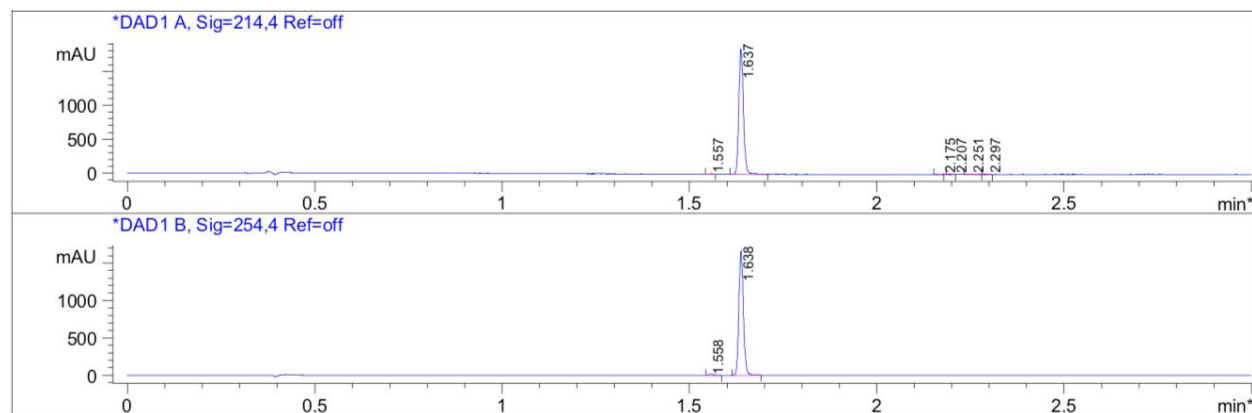
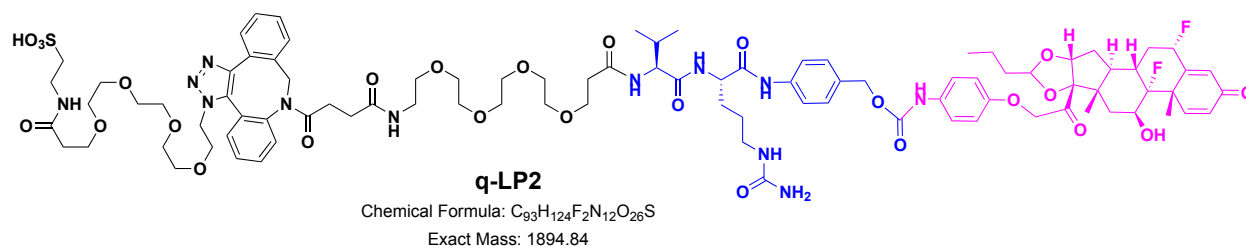
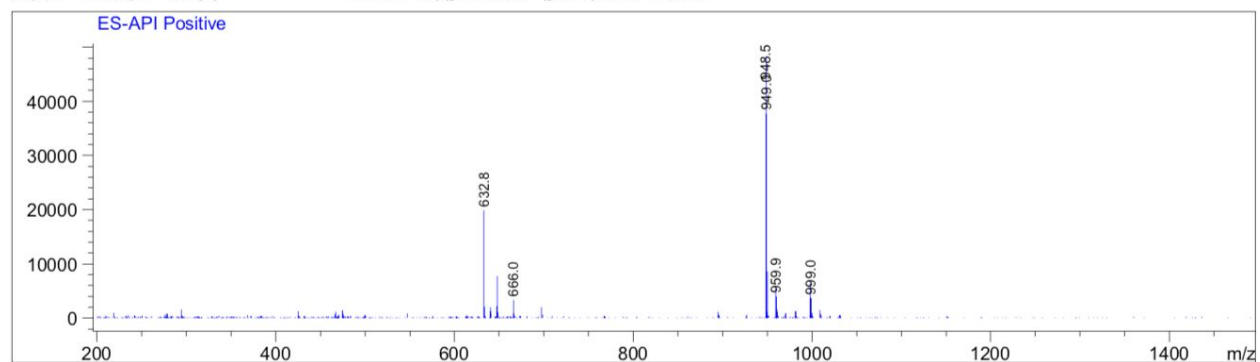


Figure S25. LC-MS of q-LP1



Ret. Time: 1.66

<<<< POSITIVE SPECTRA >>>>

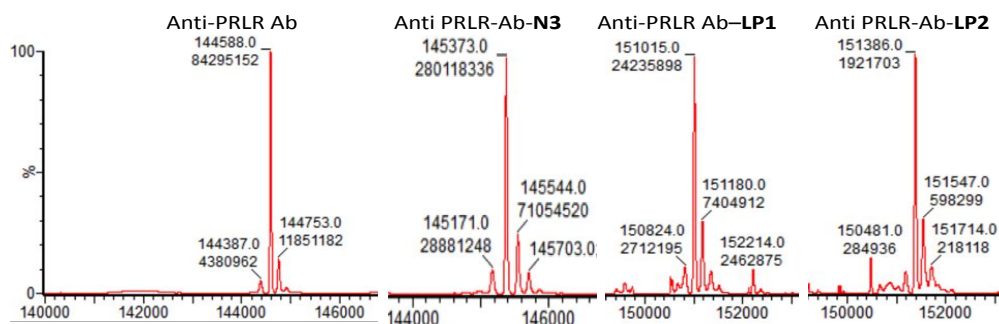


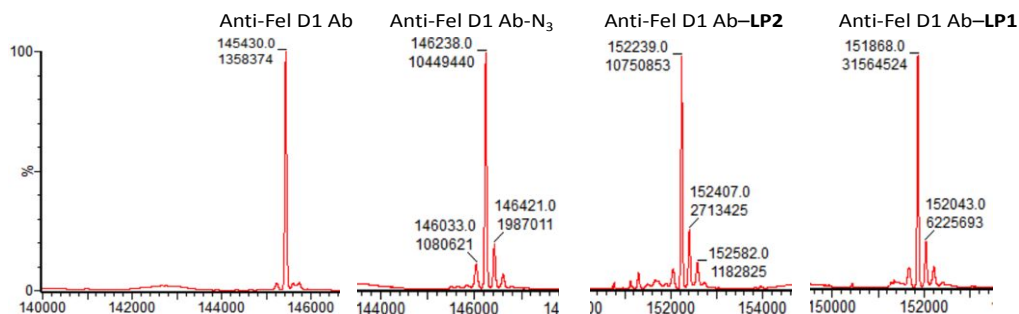
**Figure S26. LC-MS of q-LP1**

### 3. ESI-MS Spectra of Site-specific antibody drug conjugates

Intact mass spectrometry experiments were performed in positive-ion mode on a SYNAPT G2-Si instrument (Waters Corp., Manchester, UK) equipped with an electrospray (ESI) ion source. Ion-source parameters were set at 3 kV for capillary voltage, 100 V for sampling cone voltage, 800 for desolvation gas and 110°C for source temperature. Intact protein samples were separated on ACQUITY UPLC BEH C4 column (1.0 mm X 50 mm, 300 Å, 1.7 µm, Waters Corp, Milford, MA) using a 6 min linear gradient from 25-42% mobile phase B at a flow rate of 80 µL/min with the column temperature at 80°C. Mobile Phase A was 0.1% formic acid in water, while Mobile Phase B was 0.1% formic acid in acetonitrile.  $[M+2H]^{2+}$  peak of Glu-fibrinopeptide B ( $m/z$  785.8426) was used as lock mass in ESI mode. Data processing was performed using MassLynx software V4.1 (Waters Inc., 2014). The deconvolution data were obtained after smoothing, baseline subtraction, and centered using lock mass.

A sample solution for ESI-MS was prepared by the following protocol: a 0.5 mg/mL solution of mAb or ADC in deionized water was prepared in an HPLC vial and 1.5 µL of this solution (~ 0.5 µg/µL concentration) was injected for ESI-MS analysis. All mass additions to the antibodies, Ab-N<sub>3</sub> conjugates, and ADCs were confirmed by intact ESI-MS for the following samples: anti-PRLR antibody, anti-PRLR antibody-PEG<sub>3</sub>-N<sub>3</sub>, anti-PRLR antibody-LP1, anti-PRLR antibody-LP2, control antibody (anti-Fel D1 antibody), control antibody-PEG<sub>3</sub>-N<sub>3</sub>, control antibody-LP1, and control antibody-LP2 (Table S6).





Linker or Linker-Payload		Ab, Ab-N <sub>3</sub> , or GC-ADC		
Name	MW (Da)	Name	Detected Major ESI-MS m/z (Da)	Calculated DAR
		Anti-PRLR Ab	144588	-
NH <sub>2</sub> -PEG <sub>3</sub> -N <sub>3</sub>	218.3	Anti-PRLR-Ab-N <sub>3</sub>	145383	4.0
<b>LP1</b>	1405.6	Anti-PRLR Ab- <b>LP1</b>	151015	>3.9
<b>LP2</b>	1497.7	Anti-PRLR Ab- <b>LP2</b>	151386	>3.9
		Anti-Fel D1 Ab	145439	-
NH <sub>2</sub> -PEG <sub>3</sub> -N <sub>3</sub>	218.3	Anti-Fel D1 Ab-N <sub>3</sub>	146238	>3.9
<b>LP1</b>	1405.6	Anti-Fel D1 Ab- <b>LP1</b>	151884	>3.9
<b>LP2</b>	1497.7	Anti-Fel D1 Ab- <b>LP2</b>	152235	>3.9

**Table S6.** Major ESI-MS peaks of antibody (Ab), N<sub>3</sub>-tagged conjugate (Ab-N<sub>3</sub>), and site-specific antibody-GC-conjugate (GC-ADC), as well as calculated DAR values.

## 4. Bioassays

### 4.1 Cell-Free GR Binding Assay

To evaluate the ability of the novel GCs to bind to the GR receptor, a cell-free binding assay was performed using a LanthaScreen time-resolved (TR)-FRET GR Competitive Binding Assay Kit (Life Technologies, catalog # A15901). In the cell-free competitive binding assay, the Tb-anti-GST antibody indirectly labels GR ligand-binding domain by binding to the GST tag, and the test compounds compete

with the tracer-labeled control molecule to bind to the GR. The loss of FRET-signal is measured and IC<sub>50</sub> value calculated. In general, the assay was performed according to the manufacturer's instructions. Budesonide (**P1**) was used as a control reference. In the assay, a four-fold serial dilution of Budesonide and the testing compounds were prepared in 100% DMSO starting at 1000nM. A total of 60 nL of these DMSO solutions were dispensed into a 384-well assay plate, and then further diluted 166-fold in nuclear receptor buffer F with 5mM DTT and 0.1mM stabilizing peptide. Next, Fluormone GS1 Green, GR-LBD (GST) and Tb anti-GST antibody were sequentially added to a 384-well assay plate. The highest final starting concentrations of testing compounds ranged from 10μM to 0.5μM. The final DMSO concentrations in the reaction systems were all at 0.3%. The plate was then incubated at rt for 2.5 hours while being protected from light. The plate was analyzed on an Envision Multi-label Plate Reader (PerkinElmer) with excitation set at 340nm and emission filters at 520nm and 495nm. The FRET ratio was calculated as 520nm/495nm, and the IC<sub>50</sub> values determined using a four-parameter logistic equation over a 10-point response curve (GraphPad Prism).

#### 4.2 Cell-free Nuclear Receptors (NRs) binding assays panel

Payloads **P1**, **P3** and **P12** were evaluated side by side with control reference compounds against a panel of nuclear receptors via a LanthaScreen TR-FRET GR competitive binding assay format supplied by ThermoFisher. Both **P3** and **P12** demonstrated IC<sub>50</sub> >1000 nM for the panel of nuclear receptors, except PR (Table S7).

Target	Control Cmpd Name	IC <sub>50</sub> (nM)			
		Control	Bud (P1)	P3	P12
AR	R1881 (31.6 uM)	0.995	>1000	>1000	>1000
CAR	CITCO (1000 uM)	45.3	>1000	>1000	>1000
ER-alpha	17-beta-Estradiol (10 uM)	1.25	>1000	>1000	>1000

ER-beta	17-beta-Estradiol (10 uM)	2.56	>1000	>1000	>1000
FXR	GW4064 (1000 uM)	177	>1000	>1000	>1000
GR	Mometasone Furoate (100 uM)	7.85	13.5	5.94	3.022
LXR-alpha	T0901317 (50 uM)	3.05	>1000	>1000	>1000
LXR-beta	T0901317 (50 uM)	4.39	>1000	>1000	>1000
PPAR-alpha	GW7647 (50 uM)	3.26	>1000	>1000	>1000
PPAR-delta	GW501516 (100 uM)	7.35	>1000	>1000	>1000
PPAR-gamma	GW1929 (100 uM)	6.24	>1000	>1000	>1000
PR	Progesterone (100 uM)	14.1	25.5	10.1	41.3
RAR-alpha	ATRA (100 uM)	3.27	>1000	>1000	>1000
RAR-beta	ATRA (100 uM)	1.75	>1000	>1000	>1000
RAR-gamma	ATRA (100 uM)	3.24	>1000	>1000	>1000
TR-alpha	9-cis-RA (100 uM)	192	>1000	>1000	>1000
TR-beta	9-cis-RA (100 uM)	68.4	>1000	>1000	>1000
VDR	T3 (4 uM)	0.0905	>1000	>1000	>1000

**Table S7.** Cell-free NR binding activity of Budesonide, **P3** and **P12**.

### 4.3 Cell-based reporter assay

A Glucocorticoid Receptor (GR) co-activator luciferase reporter cell-based assay was used to analyze the GR activation by GCs as a function of time. A HEK293 cell line was co-transfected with a construct expressing a fusion protein of a GR ligand binding domain and the yeast Gal4 DNA domain (pBind-GR, Promega Cat# E1581), and a luciferase expression plasmid with Gal4 binding sites in the promoter region (pGL4.35[luc2P/9XGAL4UAS/Hygro], Promega, Cat# E137A). The pBind-GR vector expresses a fusion protein consisting of the yeast Gal4DNA-binding domain and the GR ligand binding domain, that

can bind to the Gal4 upstream activation sequence (UAS) in the luciferase expression vector and induce luciferase expression following GR agonist binding. This cell line was referred to as HEK293/UAS-Luc/pBIND GR cells, which can be used to evaluate the potency of GR agonist compounds. The HEK293/UAS-Luc/pBIND GR cell line was further engineered to express human full-length prolactin receptor (PRLR) and referred as HEK293/UAS-Luc/pBIND GR cell/PRLR, which is used to evaluate the potency of anti-PRLR-GR agonist ADC as well as free payload. In addition, the HEK293 cells were engineered to express human full-length PRLR only as a negative control cell line, referred as HEK293/PRLR cells.

To analyze GR activation of GCs and GC-conjugates in the assay, 20,000 /well GR reporter cells were seeded in 96-well plates (Corning #356691) in 80ul media of DMEM supplemented with 10% FBS and penicillin/streptomycin (complete media) and grown overnight at 37°C incubator with 5% CO<sub>2</sub>. For dose response curves, the serially diluted compounds (20ul ADC or testing compounds, 100nM to 5pM) were added to the cells and incubated for 72 hours at 37°C. Luciferase activity was determined by addition of One-Glo™ reagent (Promega, Cat# E6130) and relative light units (RLU) were measured on a Victor luminometer (Perkin Elmer). The EC<sub>50</sub> values were determined from a four-parameter logistic equation over a 10-point response curve using GraphPadPrism.

#### **4.4. Bystander effect assay**

To evaluate the bystander effect of the GC-conjugates, four assays were set side by side as listed below.

1. 20,000/well HEK293/UAS-Luc/pBIND GR cells in 80μl growth media
2. 20,000/well HEK293/PRLR in 80μl growth media
3. 20000/well HEK293/UAS-Luc/pBIND GR cells + 20,000/well HEK293/PRLR in 80μl growth media
4. 20,000/well HEK293/UAS-Luc/pBIND GR cell/PRLR in 80μl growth media as positive control



Cells were incubated for 72 hours at 37°C. Luciferase activity was determined by addition of One-Glo™ reagent (Promega, Cat# E6130) and relative light units (RLU) were measured on a Victor luminometer (Perkin Elmer). The EC<sub>50</sub> values were determined from a four-parameter logistic equation over a 10-point response curve using GraphPadPrism. For dose response curves, the compounds were serially diluted 3-fold in 100% DMSO, and then further diluted in the cell growth media. 20 µL of media-diluted compounds were added to the cells and the final concentrations ranged from 100 nM to 0.015 nM over 10 concentration points. To evaluate the ADC activity, GC conjugates (GC-ADCs) were 3-fold serially diluted in the cell growth media starting from 500nM. 20ul diluted ADCs were added to the reporter cells and the final concentrations ranged from 100nM to 0.015nM, with the last well as blank control containing only the assay media and 0.2% DMSO (untreated well).

## **5. ADME assays**

### **5.1 Plasma stability in human or animal plasma**

Stock solutions were prepared at 10 mM in DMSO for the test compound. Aliquots of the stock solutions were diluted to 0.02 mM in 0.05 M sodium phosphate buffer containing 0.5% BSA as the dosing solution. Then 10 µL of the dosing solutions were dosed into 90 µL of pre-warmed plasma (37°C) in singlet (n=1) in 96-well assay plates to reach a final test concentration of 2 µM. The plates were kept in a 37°C water bath for the duration of the experiment. At each time point (0, 0.25, 1, 8, 24 h), 400 µL of acetonitrile (containing internal standard) was added into corresponding wells of the assay plates. After the final time point was quenched, the assay plates were shaken on a vibrator (IKA, MTS 2/4) for 10 min (600 rpm/min) and then centrifuged at 5594 g for 15 min (Thermo Multifuge × 3R). Aliquots of the supernatant were taken and analyzed by LC-MS/MS. The peak area response ratio to internal standard (PARR) of the compounds at 0.25, 1, 8, 24 h was compared to the PARR at time 0 to determine

the percent of test compound remaining at each time point. Half-lives ( $t_{1/2}$ ) were calculated using Excel software, fitting to a single-phase exponential decay equation.

## 5.2. Caco2 assay

Caco-2 cells were obtained from American Type Culture Collection (Rockville, MD). The cells were maintained in Modified Eagle's medium (MEM), containing 10% fetal bovine serum (FCS), and 1% non-essential amino acids, in CO<sub>2</sub> at 37°C. Cells were seeded on polycarbonate filter inserts (Millipore, CAT#PSHT 010 R5) and cultured for 21–28 days prior to the transport experiments. The transepithelial electric resistance (TEER) and Lucifer Yellow permeability were checked for monolayer integrity. The testing compounds were dissolved at 10 mM in 100% dimethyl sulfoxide (DMSO), and diluted to 10 µM with the assay buffer (25 mM HEPES, pH 7.4, in Hanks Balanced Salt Solution, Invitrogen, Cat# 14025-092). The 10 µM solutions of the testing compounds were centrifuged to remove undissolved particles, and the supernatants were collected as dosing solutions. The solutions were incubated with and without 100 µM Verapamil, a Pgp inhibitor, in both the apical-to-basolateral (A-B) and basolateral-to-apical (B-A) directions at 37°C for 90 min. The initial volumes in A-B direction are 0.4 mL in donor and 0.8 mL in receiver; and in B-A direction are 0.8 mL in donor and 0.4 mL in receiver. At the end of incubation, in A-B direction, the donor samples were diluted 10-fold with the assay buffer; in B-A direction, the receiver samples were diluted 2-fold and the donor samples were diluted 10-fold with the assay buffer, and then 60 µL of each undiluted or diluted sample was mixed with 60 µL of acetonitrile (containing internal standard), respectively. All samples were analyzed by LC-MS/MS and the concentrations of the compounds were quantified by their standard curves.

Compounds measured for cell permeability and mechanism of transport using the Caco-2 permeability assay are summarized in Table S8. Budesonide displayed an efflux ratio of 1.19. Comparatively, **P3** showed low permeability ( $4.05 \times 10^{-6}$  cm/sec) in A-B direction and its efflux ratio was 8.57. Inclusion of

the P-glycoprotein (P-gp) inhibitor, verapamil, significantly reduced the efflux ratio for **P3** to 1.3. Thus, **P3** is a probable P-gp substrate. These results are consistent with previous findings that several corticosteroids (hydrocortisone, dexamethasone, methylprednisolone, cortisol and aldosterone) are substrates of P-gp.<sup>7</sup> Both **P10** and **P12** showed lower permeability either from A to B or B to A compared to Budesonide, and displayed the efflux ratios < 1, indicating both compounds are less permeable payloads with no efflux issue. All other compounds were relatively less permeable from A to B but were more permeable from B to A compared to Budesonide, resulting in higher efflux ratios.

Test Article	Mean P <sub>app</sub> ×10 <sup>6</sup> /cm·s-1		P <sub>app</sub> (B-A)/ P <sub>app</sub> (A-B)
	A-B	B-A	
<b>P1</b>	21.24	25.27	1.19
<b>P2</b>	6.81	33.66	4.94
<b>P3</b>	4.05	34.68	8.57
<b>P3+Verapamil</b>	14.1	18.4	1.31
<b>P7</b>	<1.31	21.23	>16.2
<b>P10</b>	19.26	18.04	0.94
<b>P12</b>	15.26	13.14	0.86
<b>P13</b>	<1.94	36.64	>18.9
<b>P14</b>	13.21	49.98	3.78

**Table S8.** Caco-2 permeability and efflux ratio for key compounds. cLogP was calculated based on JChemFunctions.

### 5.3. Cathepsin B Enzymatic Assay

To test a payload released from its linker-payload in a cathepsin B assay, the linker-payload stock solution (10mM in DMSO) was spiked into incubation buffer (100 mM NaOAc, 10mM dithiothreitol, pH5) to obtain a substrate solution at a concentration of 25 µM. Human liver Cathepsin B (Athena Research, USA; catalog #16-12-030102) 0.4 µg/µL in 20 mM NaOAc containing 1 mM EDTA, pH 5) was added at an

enzyme to substrate ratio of 1:50, w/w. The reaction mixture was incubated at 37 °C, and aliquots (20 µL) were taken after 4 h and quenched by adding 2 µL of acetic acid, followed by freezing at -70 °C. The digestion mixtures were analyzed by LC-MS/MS.<sup>8</sup>

Linker-payloads (**LP1** and **LP2**) and quenched linker-payloads (**q-LP1** and **q-LP2**) in CapB were incubated with and without CapB inhibitor (CA074) for 4 hours, separately; both linker-payload and free payload were evaluated using LC-MS/MS and the results are shown in main text. The unquenched linker-payloads were poorly soluble in testing media (< 0.1 mg/mL). The lower % of payload released from the corresponding linker-payload, compared to releasing from corresponding quenched linker-payload, could be contributed to the poor solubility of testing compounds in aqueous media; therefore, the data for the unquenched linker-payloads are unreliable.

## **6. In vivo evaluation of the effect of GCs on mouse model of LPS-induced TNF $\alpha$ release**

A total of 18 naive C57BL/6j mice were used in this study. The animals were male, 7 weeks with body weight of 18-20g at the initiation of the study. Animals were purchased from Shanghai Laboratory Animal Center, CAS (SLAC), and housed in ChemPartner's animal vivarium in a SPF environment. After arrival, animals were checked for health conditions including coat, extremities, orifices and abnormal signs in posture or movements, and acclimated to the environment for more than 7 days. Animals were housed 3 mice per cage in IVC polycarbonate shoebox cages in SPF environment; the environment controls for the animal room were set to maintain a temperature of 20-26°C, humidity of 40-70%, and a 12-hour light/12-hour dark cycle.

Standard chow (SLAC-M01, from Shanghai Laboratories Animal Center) and purified water (filtered, municipal water quality) were provided *ad libitum* throughout the study period. Animals were grouped randomly, allocated into 6 groups (A-F) before study initiation. Each group included 3 mice. Group A served as naive control; Group B received dexamethasone and served as positive control; Group C was

treated with **P3** and Group D-F was treated with **P12**.

All mice received LPS (Lipopolysaccharide derived from E. Coli K12 was purchased from Invivogen (San Diego, California, USA, cat# Tlr-eklps)) dissolved in PBS at a dose of 0.5mpk by i.p injection. Mice in group A received PBS, mice in group B received Dex (5mpk) and mice in group C received **P3** (5mpk) by ip injection, 2hr prior to LPS challenge; Mice in group D, E and F received **P12** at a dose of 5mpk by ip injection, 2hr, 24hr and 48hr prior to LPS challenge, respectively. Blood samples were collected at 2hr and 4hr time points post LPS challenge, into heparin containing tubes. Blood samples were centrifuged, and plasma samples were collected and stored at -80°C before analysis. The levels of TNF $\alpha$  in plasma were measured with ELISA kits (ThermoFisher Scientific, Cat#88-7324) following the standard procedures recommended by the manufacturer.

## **7. Pharmacokinetic Study protocol**

A total of 16 naive C57BL/6j mice were used in this study. The animals were male, 6-8 weeks with body weight of 19-21g at the initiation of the study. Animals were purchased from Shanghai Laboratory Animal Center, CAS (SLAC), and housed in ChemPartner's animal vivarium in a SPF environment. After arrival, animals were checked for health conditions including coat, extremities, orifices and abnormal signs in posture or movements, and acclimated to the environment for more than 7 days. Animals were housed 4 mice per cage in IVC polycarbonate shoebox cages in SPF environment; the environment controls for the animal room were set to maintain a temperature of 20-26°C, humidity of 40-70%, and a 12-hour light/12-hour dark cycle.

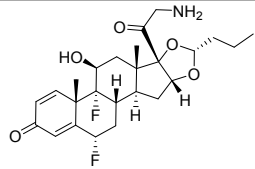
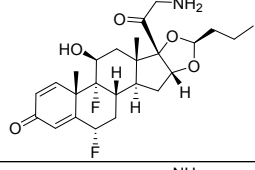
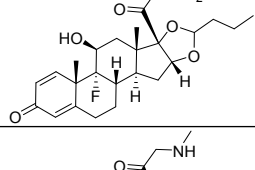
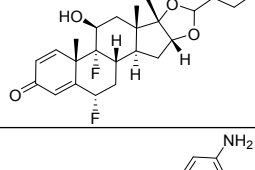
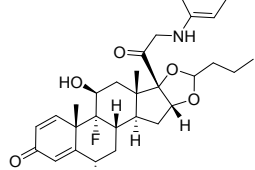
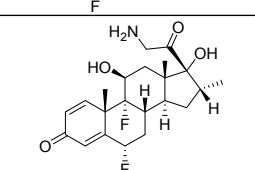
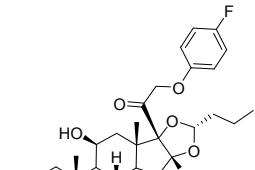
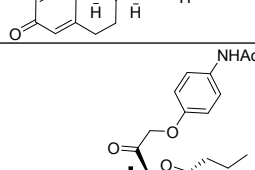
Mice in group A received PBS, mice in group B received Dex (1 mpk), mice in group C received **P3** (1 mpk) and mice in group D received **P12** (1 mpk). All test samples received by ip injection. The animals were restrained manually at the designated time points (at 0, 15 min, 1 hr, 2 hr, 4 hr, 8hr and 24 hr), approximately 30  $\mu$ L of blood sample was collected via facial vein into EDTA-K2 tubes. 20  $\mu$ L of blood

sample was diluted with 40  $\mu$ L of diH<sub>2</sub>O, vortexed for 1 min and put into dry ice temporarily and transferred into -80°C freezer for long term preservation.

## 8. Structures with SMILE formula strings

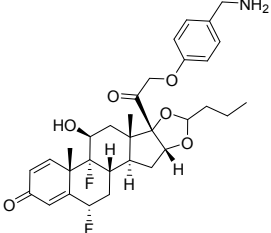
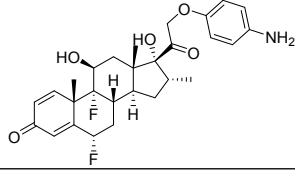
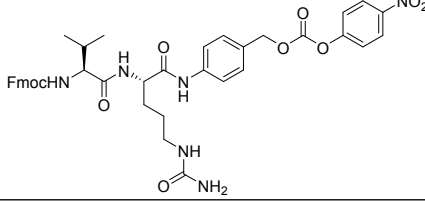
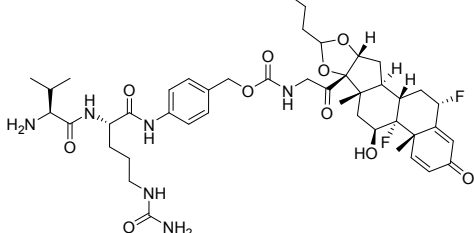
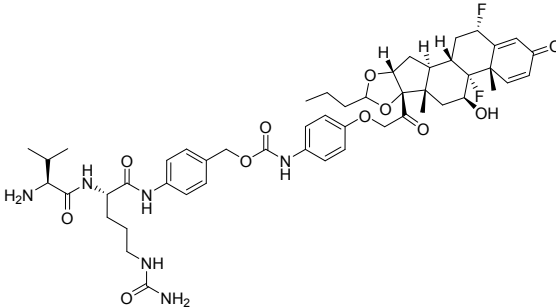
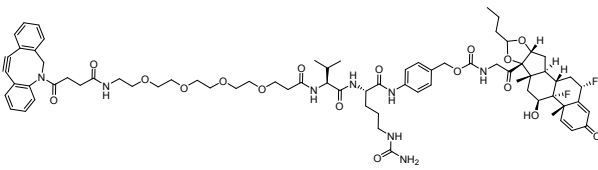
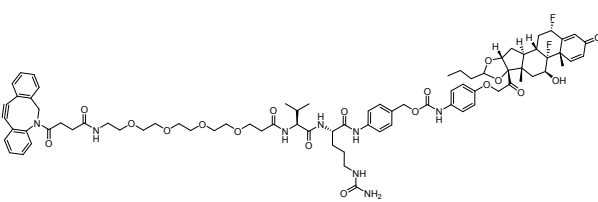
#	Structure	SMILES
IA, P1		<chem>C[C@@]12[C@](C(CO)=O)(OC(CCC)O3)[C@@]3([H])C[C@@]1([H])[C@@](CCC4=C5=O)([H])[C@]([C@@]4(C)C=C5)([H])[C@@H](O)C2</chem>
R-P1		<chem>C[C@@]12[C@](C(CO)=O)(O[C@H](CCC)O3)[C@@]3([H])C[C@@]1([H])[C@@](CCC4=CC5=O)([H])[C@]([C@@]4(C)C=C5)([H])[C@@H](O)C2</chem>
S-P1		<chem>C[C@@]12[C@](C(CO)=O)(O[C@@H](CCC)O3)[C@@]3([H])C[C@@]1([H])[C@@](CCC4=CC5=O)([H])[C@]([C@@]4(C)C=C5)([H])[C@@H](O)C2</chem>
IB		<chem>C[C@@]12[C@](C(CO)=O)(OC(CCC)O3)[C@@]3([H])C[C@@]1([H])[C@@](C[C@H](F)C4=CC5=O)([H])[C@]([C@@]4(C)C=C5)(F)[C@@H](O)C2</chem>
IC		<chem>C[C@@]12[C@](C(CO)=O)(OC(CCC)O3)[C@@]3([H])C[C@@]1([H])[C@@](CCC4=C5=O)([H])[C@]([C@@]4(C)C=C5)(F)[C@@H](O)C2</chem>
ID		<chem>C[C@@]12[C@](C(CO)=O)(O)[C@H](C)[C@@]1([H])[C@@](C[C@H](F)C3=CC4=O)([H])[C@]([C@@]3(C)C=C4)(F)[C@@H](O)C2</chem>
IE		<chem>C[C@@]12[C@](C(CO)=O)(OC(C)(C)O3)[C@@]3([H])C[C@@]1([H])[C@@](CCC4=C5=O)([H])[C@]([C@@]4(C)C=C5)(F)[C@@H](O)C2</chem>
IF		<chem>C[C@@]12[C@](C(CO)=O)(OC(C)(C)O3)[C@@]3([H])C[C@@]1([H])[C@@](C[C@H](F)C4=CC5=O)([H])[C@]([C@@]4(C)C=C5)(F)[C@@H](O)C2</chem>

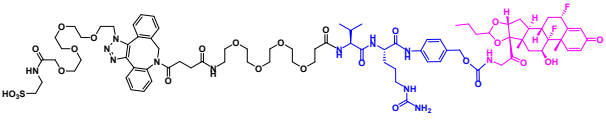
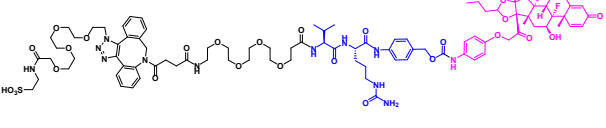
IIA		<chem>C[C@@]12[C@](C(COS(C)=O)=O)=O)(OC(CCC)O3)[C@@]3([H])C[C@@]1([H])[C@@](C(CCC4=CC5=O)([H])[C@]([C@@]4(C)=C5)([H])[C@@H](O)C2</chem>
IIB		<chem>C[C@@]12[C@](C(COS(C)=O)=O)=O)(OC(CCC)O3)[C@@]3([H])C[C@@]1([H])[C@@](C[C@H](F)C4=CC5=O)([H])[C@]([C@@]4(C)=C5)(F)[C@@H](O)C2</chem>
IIC		<chem>C[C@@]12[C@](C(COS(C)=O)=O)=O)(OC(CCC)O3)[C@@]3([H])C[C@@]1([H])[C@@](C(CCC4=CC5=O)([H])[C@]([C@@]4(C)=C5)(F)[C@@H](O)C2</chem>
IID		<chem>C[C@@]12[C@](C(COS(C)=O)=O)=O)(O)[C@H](C)C[C@@]1([H])[C@@](C[C@H](F)C3=CC4=O)([H])[C@]([C@@]3(C)C=C4)(F)[C@@H](O)C2</chem>
IIIA		<chem>C[C@@]12[C@](C(CN=[N+]=[N-])=O)(OC(CCC)O3)[C@@]3([H])C[C@@]1([H])[C@@](C(CCC4=CC5=O)([H])[C@]([C@@]4(C)=C5)([H])[C@@H](O)C2</chem>
IIIB		<chem>C[C@@]12[C@](C(CN=[N+]=[N-])=O)(OC(CCC)O3)[C@@]3([H])C[C@@]1([H])[C@@](C[C@H](F)C4=CC5=O)([H])[C@]([C@@]4(C)=C5)(F)[C@@H](O)C2</chem>
IIIC		<chem>C[C@@]12[C@](C(CN=[N+]=[N-])=O)(OC(CCC)O3)[C@@]3([H])C[C@@]1([H])[C@@](C(CCC4=CC5=O)([H])[C@]([C@@]4(C)=C5)(F)[C@@H](O)C2</chem>
IIID		<chem>C[C@@]12[C@](C(CN=[N+]=[N-])=O)(O)[C@H](C)C[C@@]1([H])[C@@](C[C@H](F)C3=CC4=O)([H])[C@]([C@@]3(C)C=C4)(F)[C@@H](O)C2</chem>
P2		<chem>C[C@@]12[C@](C(CN)=O)(OC(CCC)O3)[C@@]3([H])C[C@@]1([H])[C@@](C(CCC4=CC5=O)([H])[C@]([C@@]4(C)=C5)([H])[C@@H](O)C2</chem>
P3		<chem>C[C@@]12[C@](C(CN)=O)(OC(CCC)O3)[C@@]3([H])C[C@@]1([H])[C@@](C[C@H](F)C4=CC5=O)([H])[C@]([C@@]4(C)=C5)(F)[C@@H](O)C2</chem>

R-P3		<chem>C[C@@]12[C@](C(CN)=O)(O[C@H](CCC)O3)[C@@]3([H])C[C@@]1([H])[C@@](C[C@H](F)C4=CC5=O)([H])[C@]([C@@]4(C)C=C5)(F)[C@@H](O)C2</chem>
S-P3		<chem>C[C@@]12[C@](C(CN)=O)(O[C@@H](CCC)O3)[C@@]3([H])C[C@@]1([H])[C@@](C[C@H](F)C4=CC5=O)([H])[C@]([C@@]4(C)C=C5)(F)[C@@H](O)C2</chem>
P4		<chem>C[C@@]12[C@](C(CN)=O)(OC(CCC)O3)[C@@]3([H])C[C@@]1([H])[C@@](CCC4=C5=O)([H])[C@]([C@@]4(C)C=C5)(F)[C@@H](O)C2</chem>
P5		<chem>C[C@@]12[C@](C(CNC)=O)(OC(CCC)O3)[C@@]3([H])C[C@@]1([H])[C@@](C[C@H](F)C4=CC5=O)([H])[C@]([C@@]4(C)C=C5)(F)[C@@H](O)C2</chem>
P6		<chem>C[C@@]12[C@](C(CNC3=CC=C(N)C=C3)=O)(OC(CCC)O4)[C@@]4([H])C[C@@]1([H])[C@@](C[C@H](F)C5=CC6=O)([H])[C@]([C@@]5(C)C=C6)(F)[C@@H](O)C2</chem>
P7		<chem>O=C(CN)[C@]([C@]([H])(C)C1)(O)[C@]2(C)[C@]1([H])[C@]3([H])C[C@H](F)C([C@@](C=C4)(C)[C@@]3(F)[C@@H](O)C2)=CC4=O</chem>
P8		<chem>C[C@@]12[C@](C(COC3=CC=C(F)C=C3)=O)(O[C@H](CCC)O4)[C@@]4([H])C[C@@]1([H])[C@@](CCC5=CC6=O)([H])[C@]([C@@]5(C)C=C6)([H])[C@@H](O)C2</chem>
P9		<chem>C[C@@]12[C@](C(COC3=CC=C(NC(C)=O)C=C3)=O)(O[C@H](CCC)O4)[C@@]4([H])C[C@@]1([H])[C@@](CCC5=CC6=O)([H])[C@]([C@@]5(C)C=C6)([H])[C@@H](O)C2</chem>



P10		<chem>C[C@@]12[C@](C(COC3=CC=C(N)C=C3)=O)(OC(CCC)O4)[C@@]4([H])C[C@@]1([H])[C@@](CC([H])C5=CC6=O)([H])[C@]([C@@]5(C)C=C6)([H])[C@@H](O)C2</chem>
R-P10		<chem>C[C@@]12[C@](C(COC3=CC=C(N)C=C3)=O)(O[C@H](CCC)O4)[C@@]4([H])C[C@@]1([H])[C@@](CC([H])C5=CC6=O)([H])[C@]([C@@]5(C)C=C6)([H])[C@@H](O)C2</chem>
S-P10		<chem>C[C@@]12[C@](C(COC3=CC=C(N)C=C3)=O)(O[C@@H](CCC)O4)[C@@]4([H])C[C@@]1([H])[C@@](CC([H])C5=CC6=O)([H])[C@]([C@@]5(C)C=C6)([H])[C@@H](O)C2</chem>
P11		<chem>C[C@@]12[C@](C(COC3=CC(N)=CC=C3)=O)(OC(CCC)O4)[C@@]4([H])C[C@@]1([H])[C@@](C[C@H](F)C5=CC6=O)([H])[C@]([C@@]5(C)C=C6)(F)[C@@H](O)C2</chem>
P12		<chem>C[C@@]12[C@](C(COC3=CC=C(N)C=C3)=O)(OC(CCC)O4)[C@@]4([H])C[C@@]1([H])[C@@](C[C@H](F)C5=CC6=O)([H])[C@]([C@@]5(C)C=C6)(F)[C@@H](O)C2</chem>
R-P12		<chem>C[C@@]12[C@](C(COC3=CC=C(N)C=C3)=O)(O[C@H](CCC)O4)[C@@]4([H])C[C@@]1([H])[C@@](C[C@H](F)C5=CC6=O)([H])[C@]([C@@]5(C)C=C6)(F)[C@@H](O)C2</chem>
S-P12		<chem>C[C@@]12[C@](C(COC3=CC=C(N)C=C3)=O)(O[C@@H](CCC)O4)[C@@]4([H])C[C@@]1([H])[C@@](C[C@H](F)C5=CC6=O)([H])[C@]([C@@]5(C)C=C6)(F)[C@@H](O)C2</chem>

P13		<chem>C[C@@]12[C@](C(COC3=CC=C(CN)C=C3)=O)(OC(CCC)O4)[C@@]4([H])C[C@@]1([H])[C@@](C[C@H](F)C5=CC6=O)([H])[C@]([C@@]5(C)C=C6)(F)[C@@H](O)C2</chem>
P14		<chem>C[C@@]12[C@](C(COC3=CC=C(CN)C=C3)=O)(O)[C@H](C)C[C@@]1([H])[C@@](C[C@H](F)C4=CC5=O)([H])[C@]([C@@]4(C)C=C5)(F)[C@@H](O)C2</chem>
IV		<chem>O=C(NC(C=C1)=CC=C1COC(OC2=CC=C([N+])([O-])=O)C=C2)=O)[C@H](CCCNC(N)=O)NC([C@H](C(C)C)NC(OCC3C(C=CC=C4)=C4C5=C3C=CC=C5)=O)=O</chem>
VA		<chem>O=C(NC(C=C1)=CC=C1COC(NCC([C@]([C@@]2([H])C3)(OC(CCC)O2)[C@]4(C)[C@]3([H])[C@]5([H])C[C@H](F)C([C@@](C=C6)(C)[C@](F)5[C@@H](O)C4)=CC6=O)=O)[C@H](CCCNC(N)=O)NC([C@H](C(C)C)N)=O</chem>
VB		<chem>O=C(NC(C=C1)=CC=C1COC(NC(C=C2)=CC=C2OCC([C@]([C@@]3([H])C4)(OC(CCC)O3)[C@]5(C)[C@]4([H])[C@]6([H])C[C@H](F)C([C@@](C=C7)(C)[C@]6(F)[C@@H](O)C5)=CC7=O)=O)[C@H](CCCNC(N)=O)NC([C@H](C(C)C)N)=O</chem>
LP1		<chem>O=C(N[C@@H](C(C)C)C(N[C@@H](CCCN(C(N)=O)C(NC(C=C1)=CC=C1COC(NCC([C@]([C@@]2([H])C3)(OC(CCC)O2)[C@]4(C)[C@]3([H])[C@]5([H])C[C@H](F)C([C@@](C=C6)(C)[C@](F)5[C@@H](O)C4)=CC6=O)=O)=O)=O)CCOCCOCCOCCOCCN(CCC(N7CC(C=CC=C8)=C8C#CC9=C7C=CC=C9)=O)=O</chem>
LP2		<chem>O=C(N[C@@H](C(C)C)C(N[C@@H](CCCN(C(N)=O)C(NC(C=C1)=CC=C1COC(NC(C=C2)=CC=C2OCC([C@]([C@@]3([H])C4)(OC(CCC)O3)[C@]5(C)[C@]4([H])[C@]6([H])C[C@H](F)C([C@@](C=C7)(C)[C@]6(F)[C@@H](O)C5)=CC7=O)=O)=O)=O)CCOCC</chem>

		<chem>OCCOCCOCCNC(CCC(N8CC(C=CC=C9)=C9C#CC%10=C8C=CC=C%10)=O)=O</chem>
q-LP1		<chem>O=C(NCCOCCOCCOCCOCC(CN[C@@H](C(C)C)C(N[C@@H](CCCNC(N)=O)C(NC1=CC=C(COC(NCC([C@@]23[C@@](OC(CCC)O3)([H])C[C@@]4([H])[C@]([C@]5(F)[C@@H](O)C[C@@]42C)([H])C[C@H](F)C([C@]5(C)C=C6)=CC6=O)=O)=O)C=C1)=O)=O)CCC(N7CC(C=CC=C8)=C8C(N(CCOCCOCCOCCOCC(NCCS(=O)(O)=O)=O)N=N9)=C9C%10=C7C=CC=C%10)=O</chem>
q-LP2		<chem>CCCC1O[C@]2([H])C[C@@]3([H])[C@]([C@]4(F)[C@@H](O)C[C@]3(C)[C@]2(C(CO C5=CC=C(NC(OCC(C=C6)=CC=C6NC([C@H](CCCNC(N)=O)NC([C@H](C(C)C)NC(CCOCCOCCOCCOCCOCCOCC(NCCS(=O)(O)=O)=O)N=N9)=C9C%10=C7C=CC=C%10)=O)=O)C=C5)=O)O1)([H])C[C@H](F)C([C@]4(C)C=C%11)=CC%11=O</chem>

## 9. References

- [1] The software of Schrödinger Release 2017-3 can be accessed on <https://www.schrodinger.com/>: (a) <https://www.schrodinger.com/drug-discovery>; (b) <https://www.schrodinger.com/LigPrep/>; (c) <https://www.schrodinger.com/jp/protein-preparation-wizard>; (d) <https://www.schrodinger.com/Induced-Fit/>; (e) <https://www.schrodinger.com/Induced-Fit/>.
- [2] The PyMOL Molecular Graphics System, Version 1.8 Schrödinger, LLC.; <https://www.schrodinger.com/pymol/>
- [3] Hemmerling, M.; Nilsson, S.; Edman, K.; Eirefelt, S.; Russell, W.; Hendrickx, R.; Johnsson, E.; Kärrman Mårdh, C.; Berger, M.; Rehwinkel, H.; Abrahamsson, A.; Dahmén, J.; Eriksson, A. R.; Gabos, B.; Henriksson, K.; Hossain, N.; Ivanova, S.; Jansson, A. H.; Jensen, T. J.; Jerre, A.; Johansson, H.; Klingstedt, T.; Lepistö, M.; Lindsjö, M.; Mile, I.; Nikitidis, G.; Steele, J.; Tehler, U.; Wissler, L.; Hansson, T.; Selective Nonsteroidal Glucocorticoid Receptor Modulators for the Inhaled Treatment of Pulmonary Diseases. *J. Med. Chem.* **2017**, *60*, 8591-8605.

- [4] Brattsand, R.; Thalén, A.; Roempke, K.; Källström, L.; Gruvstad, E.; Influence of 16a,17a-acetal substitution and steroid nucleus fluorination on the topical to systemic activity ratio of glucocorticoids. *J. Steroid Biochem.* **1982**, *16*, 779-786.
- [5] Thalen, A.; Epimers of Budesonide and related corticosteroids. III. Synthesis and structure elucidation by carbon-13 and proton nuclear magnetic resonance spectroscopy. *Acta Pharm. Suec.* **1987**, *24*, 97-114.
- [6] Felletti, S.; Ismail, O. H.; Luca, C. D.; Costa, V.; Gasparrini, F.; Pasti, L.; Marchetti, N.; Cavazzini, A.; Catani, M.; Recent achievements and future challenges in supercritical fluid chromatography for the enantioselective separation of chiral pharmaceuticals. *Chromatographia* **2019**, *82*, 65-75.
- [7] Crowe, A.; Tan, A. M.; Oral and inhaled corticosteroids: Differences in P-glycoprotein (ABCB1) mediated efflux. *Toxicology and Applied Pharmacology* **2012**, *260* (3), 294-302.
- [8] Szabo, I.; Manea, M.; Orban, E.; Csampai, A.; Bosze, S.; Szabo, R.; Tejeda, M.; Gaal, D.; Kapuvári, B.; Przybylski, M.; Hudecz, F.; Mezo, G.; Development of an oxime bond containing daunorubicin-gonadotropin-releasing hormone-III conjugate as a potential anticancer drug. *Bioconjugate Chem.* **2009**, *20*, 656–665.